

Use of Gene Dosage Effects for a Whole-Genome Screen To Identify *Mycobacterium marinum* Macrophage Infection Loci[∇]

Bonggoo Park,[‡] Selvakumar Subbian, Sahar H. El-Etr,[†] Suat L. G. Cirillo, and Jeffrey D. Cirillo*

Department of Microbial and Molecular Pathogenesis, Texas A&M University System Health Sciences Center,
467 Reynolds Medical Building, College Station, Texas 77843-1114

Received 13 December 2007/Returned for modification 17 January 2008/Accepted 17 April 2008

We recently identified two loci, *mel1* and *mel2*, that affect macrophage infection by *Mycobacterium marinum*. The ability of these loci to confer enhanced infection in trans is presumably due to gene dosage effects since their presence on plasmids increases expression from five- to eightfold. Reasoning that this phenomenon would allow identification of other mycobacterial genes involved in macrophage infection, we conducted a screen of an *M. marinum* DNA library that provides 2.6-fold coverage of the entire genome for clones that affect macrophage infection. Our preliminary screen identified 76 plasmids that carry loci affecting macrophage infection. We eliminated plasmids that do not confer the expected phenotype when retransformed (70%), that have identical physical maps (5%), or that carry either of the *mel1* or *mel2* loci (14%) from further consideration. Four loci that confer enhanced infection (*mel*) and four that confer repressed infection (*mrl*) of macrophages were identified, and two of each group were chosen for detailed analysis. Saturating transposon mutagenesis was used to identify the loci responsible, and *M. marinum* mutants were constructed in the genes involved. We expect these genes to provide insight into how mycobacteria parasitize macrophages, an important component of innate immunity.

Mycobacterium marinum is a natural pathogen of humans (41, 49, 57), fish, and amphibians (18), causing more than 150 human infections each year in the United States alone (29). Although *M. marinum* causes primarily skin lesions on the extremities in humans (19), it causes a systemic tuberculous disease in fish and amphibians (30, 73, 101). *M. marinum* infections result in granuloma formation, whether in humans, mice, fish, or amphibians (18–20, 101). Granuloma formation occurs because macrophages become infected and allow growth of *M. marinum* during disease (19, 74) and in laboratory model systems (7, 33, 69, 81). These characteristics of infections, along with the relative ease of manipulation (3, 37, 82, 88), rapid growth rate compared to other pathogenic mycobacteria (18), and the presence of numerous useful virulence models (11, 20, 27, 33, 84, 89, 92), have aroused great interest in the molecular mechanisms of *M. marinum* pathogenesis. Significant progress has been made toward understanding *M. marinum* evolution (106), trafficking (7, 86, 98), secretion (1, 36), gene regulation (6, 82), photochromogenicity (35, 83), cell wall synthesis (3, 24, 37), granuloma formation (23, 27, 97), resistance to oxidative species (78, 79, 95, 96), and mechanisms of macrophage infection (32, 38, 66).

As a means to better understand the molecular mechanisms of macrophage infection by *M. marinum*, we recently screened

a genomic library for loci that have the ability to confer enhanced macrophage infection to *M. smegmatis* (32), a non-pathogenic mycobacterial species that does not infect macrophages efficiently. We identified two *M. marinum* loci, *mel1* and *mel2*, that confer enhanced macrophage infection to both *M. smegmatis* and *M. marinum*. The phenotypic effect of cosmids containing *mel* loci in *M. marinum* suggests that gene dosage effects, due to the resulting gene copy number, increase the expression of these genes above basal levels and thereby increase the efficiency of macrophage infection. This conclusion is consistent with our previous observations, and that of other groups, that many pathogenic bacteria, including other mycobacteria, are more virulent when grown in eukaryotic cells than when grown in laboratory medium (12–15, 65). If these hypotheses are correct, gene dosage effects could be used to identify additional genes that play a role in macrophage infection through screening a *M. marinum* genomic library in wild-type *M. marinum* for enhanced macrophage infection under standard laboratory growth conditions.

In the present study, we demonstrate the feasibility of this approach by evaluating the efficiency of macrophage infection under different stages of *M. marinum* growth when cultured in laboratory medium. We also confirm the ability of the *mel1* and *mel2* loci to confer enhanced infection of macrophages to *M. marinum* when carried on plasmids and evaluate the ability of gene dosage effects to increase levels of *melF* expression, the first gene in the *mel2* locus. These observations led us to conduct a whole-genome screen in *M. marinum* for macrophage infection loci using gene dosage effects. We identified a total of eight loci: four that enhance and four that repress macrophage infection. Detailed characterization of four of these loci resulted in the identification of at least seven newly described genes that play a role in macrophage infection by *M. marinum*. These observations suggest, for the first time, that *M.*

* Corresponding author. Mailing address: Department of Microbial and Molecular Pathogenesis, Texas A&M University System Health Sciences Center, 467 Reynolds Medical Building, College Station, TX 77843-1114. Phone: (979) 458-0778. Fax: (979) 845-3479. E-mail: jdcirillo@medicine.tamhsc.edu.

[‡] Present address: Lawrence Livermore National Lab, Biosciences and Biotechnology Division, Livermore, CA 94550.

[†] Present address: Cedars-Sinai Medical Center, Immunology Research Institute, Los Angeles, CA 90048.

[∇] Published ahead of print on 28 April 2008.

marinum has the ability to modulate infection of macrophages in both a positive and negative manner, which may play a previously under appreciated role in pathogenesis.

MATERIALS AND METHODS

Strains and growth conditions. *M. marinum* strain M, a clinical isolate obtained from the skin of a patient (81), was used in these studies. *M. marinum* strains were grown at 33°C in 7H9 broth (Difco, Detroit, MI) supplemented with 0.5% glycerol, 10% albumin-dextrose complex (ADC), and 0.25% Tween 80 (M-ADC-TW) for 5 days. Cultures were grown to an optical density at 600 nm (OD₆₀₀) of 0.5 (except where specifically indicated otherwise), mixed vigorously using a vortex for 1 min, passed through a 27-gauge syringe needle twice, and allowed to settle for 5 min prior to taking aliquots from the top half of the culture for use in assays to ensure single-cell suspensions were used in all assays. The number of viable bacteria was determined for each assay using the Live/Dead assay (Molecular Probes, Eugene, OR) and by plating dilutions for CFU on 7H9 (M-ADC) agar (Difco). All inocula used were >99% viable. *Escherichia coli* strain XL1-Blue (Stratagene) was grown in Luria-Bertani (LB) medium (Difco) at 37°C. Where appropriate, kanamycin or chloramphenicol were added at a concentration of 25 µg/ml (*E. coli*) or 10 µg/ml (*M. marinum*). X-Gal (5-bromo-4-chloro-3-indolyl-β-D-galactopyranoside) was added at concentrations of 40 µg/ml in *E. coli* and 80 µg/ml in *M. marinum*, when needed.

Monocytic cell lines and culture conditions. The murine macrophage cell lines RAW 264.7 (ATCC CRL-2278) and J774A.1 (ATCC TIB67) were maintained in 5% CO₂ at 37°C in high-glucose Dulbecco modified Eagle medium (Gibco, Bethesda, MD) supplemented with 10% heat-inactivated fetal bovine serum (Gibco) and 2 mM L-glutamine. The human monocytic cell line THP-1 (ATCC TIB202) was maintained at 37°C and 5% CO₂ in RPMI medium supplemented with 10% heat-inactivated fetal bovine serum and 2 mM L-glutamine. The adherent carp monocytic/macrophage cell line CLC (European Collection of Cell Cultures no. 95070628) was maintained at 28°C and 5% CO₂ using high-glucose minimal essential medium (Gibco) supplemented with 1% nonessential amino acids, 10% heat-inactivated fetal bovine serum (Gibco), and 2 mM L-glutamine. Cell viability was determined for all cell lines by exclusion of trypan blue as described previously (95). The cell viability for all cells in all assays was >90%.

***M. marinum* growth phase and entry assays.** *M. marinum* was inoculated at an OD₆₀₀ of 0.01 (~3 × 10⁶ CFU/ml) in 100 ml of M-ADC-TW and grown at 33°C. Aliquots were taken at various time points, the OD₆₀₀ was measured, and dilutions were plated on M-ADC plates to determine CFU. At each time point entry assays were performed using the bacteria in the aliquots at a multiplicity of infection (bacteria/host cells) of 10. Entry assays were carried out as described previously for J774A.1, RAW 264.7, and THP-1 cells (32) and for CLC cells (33). Basically, approximately 10⁶ cells were infected for 30 min, washed twice with phosphate-buffered saline (PBS), and incubated in fresh medium for 2 h with 200 µg of amikacin/ml at 37°C to kill extracellular bacteria. The cells were then washed with PBS, lysed with 0.1% Triton X-100, and dilutions were plated on M-ADC to determine the intracellular CFU. The percent entry was then calculated as follows: (CFU_{intracellular}/CFU_{inoculum}) × 100.

Determination of RNA transcript levels. Reverse transcription-PCR (RT-PCR) was used to quantify levels of 16S rRNA, *melf*, *melM*, *melO*, and *melP* transcription in different mycobacterial strains within the linear amplification range, as described previously (96). Basically, 300 to 500 ng of DNase-treated, total bacterial RNA was mixed with gene-specific reverse primers (Table 1), deoxynucleoside triphosphate mix and 40 U of RNaseOUT, incubated at 65°C for 5 min, and placed on ice prior to use. The annealed primers were extended with 15 U of ThermoScript RT at 55°C for 60 min, followed by heat inactivation of the enzyme at 85°C for 5 min. The residual, nontranscribed RNA were removed with 2 U of *E. coli* RNase H at 37°C for 20 min. Then, 2 µl of the cDNA was used in PCR amplification with 1 mM appropriate forward and reverse primers (Table 1) and 5 U of Thermopol enzyme (NEB) in a total volume of 50 µl. The amplified products were analyzed by 0.8% agarose gel electrophoresis, and the products for the appropriate dilutions of each target within the linear amplification range were measured by densitometry semiquantitatively by using a ChemiDoc XRS (Bio-Rad) and QuantityOne software.

In the case of quantitative RT-PCR, cDNA was synthesized by using SuperScript II and random decamers (Ambion). The primers corresponding to 16S rRNA, *sigA*, *melf*, *melM*, *melN*, *melO*, *melP*, and *mrlI* (Table 1) were used to amplify 10 ng of cDNA with Sybr GreenER qPCR SuperMix Universal (Invitrogen) in an Applied Biosystems 7500 RT-PCR system in triplicate. Products were verified by agarose gel electrophoresis after amplification. Relative quantities of RNA transcripts were calculated by using the comparative C_T method with 16S

TABLE 1. Oligonucleotides

Name ^a	Target gene ^b	Sequence (5'–3')
MelFF	<i>melf</i>	CAGAAGACGCGATCACGGCG
MelFR		GGGTCGGCGAACACTTCACC
MelMF	<i>melM</i>	CCTGGACCTGCCGCGCCTTG
MelMR		GTTACAGCGCCGACGCGTGG
MelNF	<i>melN</i>	CCCAGCGGCACATCCCGGTG
MelNR		CGCTGTGGTGGGCGTAGCCG
MelOF	<i>melO</i>	GACCCCTGCGCACCTCGCCG
MelOR		CCGTCTGACCATCCGACCCG
MelPF	<i>melP</i>	CCCAACACTGTCCACCCTGG
MelPR		CGTTGGCGGTGCAGGTCATC
MrlIF	<i>mrlI</i>	CCCGTTGGGACTGGCTAC
MrlIR		GCCGAGGAGGTGCTATGA
SigAF	<i>sigA</i>	CCTCAACACTGTCCGCGCCG
SigAR		GGCGCAGGTTGGCTCCAGC
rRNAF	16S rRNA	AGAGTTTGATCCTGGCTCAG
rRNAR		CACGCTCACAGTTAAGCTGT
MelDF	<i>melD</i>	CTAGCTCAGCTCGGTAGTC
MelDR		GCAAGAACCTGCATCTGGCC
MelF2F	<i>melf</i>	TCGGAATATTCCTCATGCCG
MelF2R		GTTGGTCTTCGGTCCAGATC
MelLF	<i>melL</i>	TATAGTACGCAACCAAGCA GCAATGACAG
MelLR		TATATTAATTAACAACATCA GGCCCAAGAAAG
MrlACF	<i>mrlA-C</i>	TATATTAATTAACGGCTGACT TCCCGGATTCC
MrlACR		TATATTAATTAACGAGGCCAT GGTCGACCAGG
MrlFOF	<i>mrlF-O</i>	TATATTAATTAAGCCACCG GACATACGAC
MrlFOR		TATAAGTACTGTGCCGTTCCC ACAGTCC
MrlJOF	<i>mrlJ-O</i>	TATATTAATTAACCGTCGAG GTGATCGTG
MrlJOR		TATAAGTACTGTGCCGTTCCC ACAGTCC

^a Suffixes: F, forward primer; R, reverse primer.

^b That is, the target gene mRNA transcript for RT-PCR analyses or PCR or target genes for the construction of the complementation constructs pJDC117 (*melL*), pJDC119 (*mrlA-C*), pJDC120 (*mrlF-O*), and pJDC121 (*mrlJ-O*). Oligonucleotides are listed as primer pairs. Reverse primers were used for cDNA synthesis, and both forward and reverse primers were used for RT-PCR and PCR cloning.

rRNA as an internal standard. The fold increase in expression was calculated by the 2^{-ΔΔCT} method, as described previously (9).

Construction of an arrayed *M. marinum* total DNA cosmid library in *M. marinum*. A contiguous fragment library was constructed in the cosmid pJDC16 from *M. marinum* total DNA as described previously (32). The average fragment size for DNA inserts in this library were between 40 and 50 kbp in length. Approximately 20,000 cosmid clones from this library in *E. coli* were pooled and plated for individual colonies on LB agar plus kanamycin. A total of 384 individual colonies were picked and grown in 100 µl of LB plus kanamycin in 96-well microtiter dishes. A replica was made of this arrayed library, and both samples were stocked in 50% glycerol and stored at -80°C until use. The randomness and integrity of the library was confirmed by restriction analysis of 20 random cosmids from the library. Of the 20 clones, 100% carried the appropriate size of insert and displayed unique PstI physical maps. Plasmid was prepared from each clone in the entire *E. coli* library and used to transform *M. marinum* by electroporation as described previously (16). One clone from each transformation was grown in M-ADC-TW plus kanamycin and stored in 50% glycerol at -80°C in 96-well microtiter dishes until use.

***M. marinum* whole-genome screen for loci affecting macrophage infection.** The entire arrayed *M. marinum* genomic library carried by *M. marinum* was screened for the effects of gene dosage on macrophage infection in RAW 264.7 cells. Groups of between 5 and 12 clones from the library were grown separately and evaluated in all assays, along with wild-type *M. marinum* and *M. marinum* that carries the vector backbone pJDC16. All cultures for assays were grown in 1 ml

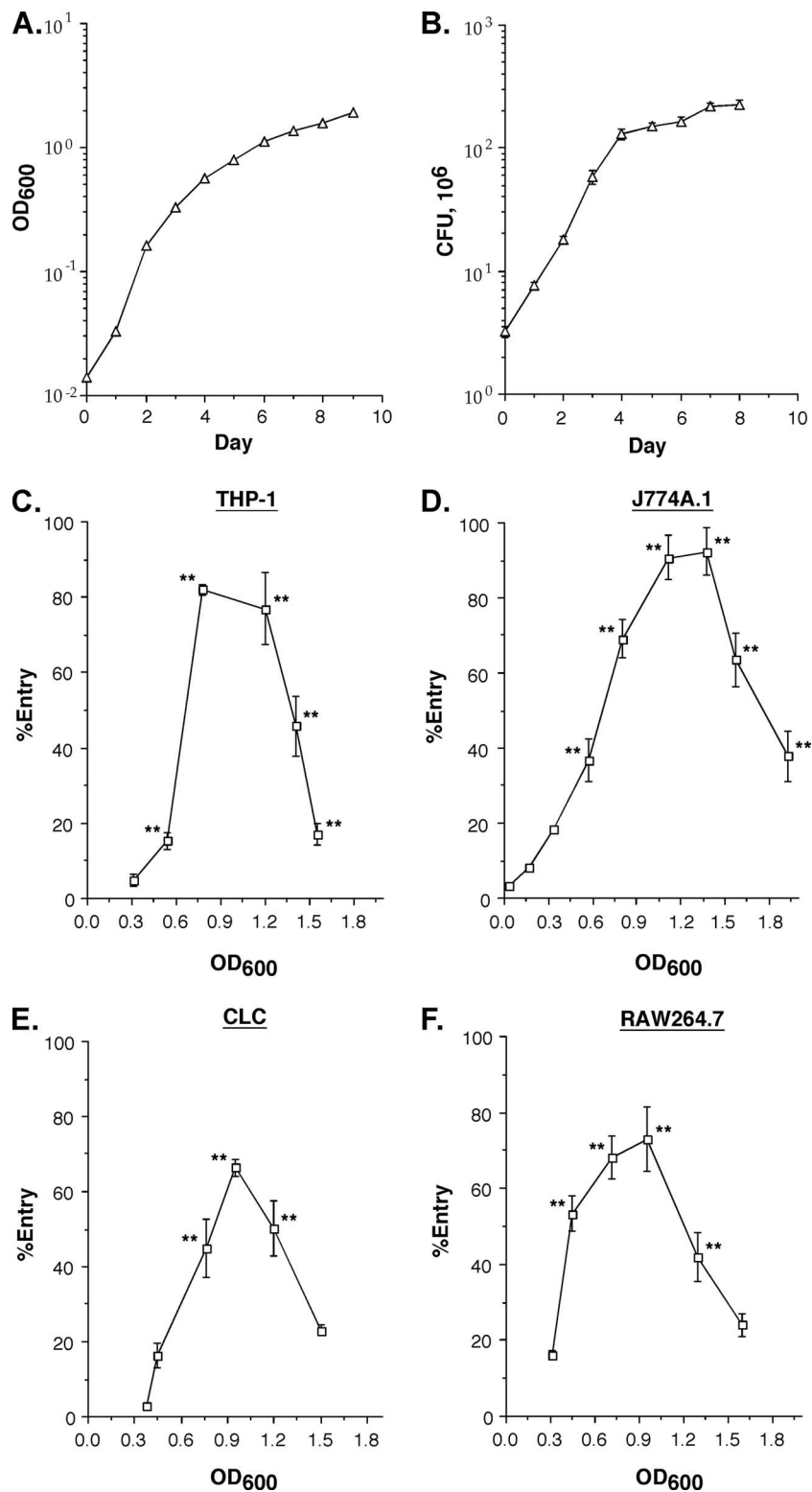


FIG. 1. Growth of *M. marinum* in M-ADC-TW broth as determined by OD₆₀₀ (A) and CFU (B). The percentages of the *M. marinum* inoculum that enters human monocytic/macrophage THP-1 (C), murine macrophage J774A.1 (D), and RAW 264.7 (F) cell lines and the fish monocytic/macrophage CLC (E) cell line when grown to different optical densities are also shown. Each data point indicates the mean, and error bars indicate the standard deviation of triplicate samples from a representative experiment of two independent experiments. **, $P < 0.01$ compared to the means of data at OD₆₀₀ = 0.3 to 0.5.

of M-ADC-TW plus kanamycin and without kanamycin for the wild type without vector. Monolayers of 10^6 RAW 264.7 cells were then infected with approximately 10^7 bacteria from each culture for 30 min at 37°C in 24-well tissue culture dishes, washed three times with warm PBS, and lysed with 0.1% Triton X-100, and dilutions were plated on M-ADC to determine cell-associated CFU. The percent cell association was then calculated as follows: $(\text{CFU}_{\text{intracellular}}/\text{CFU}_{\text{inoculum}}) \times 100$. In the initial screen, all assays were carried out in triplicate, and two independent assays were carried out with each of the 384 clones in the library. All data were normalized to the median cell association for all assays, arbitrarily set to 1. Positive clones were chosen based on their significantly ($P < 0.05$) different, either increased or decreased, cell association from the median. Cosmids were then purified from all 76 positive clones, transferred to *E. coli*, physically mapped with PstI and NotI, and screened for the presence of *mel1* or *mel2* genes (32) by PCR using the oligonucleotide pairs MelDF-MelDR or MelF2F-MelF2R, respectively. The cosmids were retransformed into *M. marinum* by electroporation and reassayed for the effects on RAW 264.7 cell association in three independent assays in triplicate. Cosmid clones that consistently conferred a difference in macrophage infection in cell association assays were chosen for determination of the genes involved.

Identification of mycobacterial enhanced and repressed macrophage infection loci. Four cosmids were chosen for detailed characterization as described previously (32): two that confer enhanced macrophage infection (*mel*) and two that confer repressed macrophage infection (*mrl*) to *M. marinum*. All four cosmids were mutagenized by saturating transposon mutagenesis with the chloramphenicol-resistant mini-*Mu* transposon as recommended by the manufacturer of the system (Finnzymes). Each mutagenized cosmid was transformed into *M. marinum*, and the resulting transformants were evaluated in three independent RAW 264.7 cell association assays in triplicate. Cosmids that no longer confer the phenotype of the original cosmid, due to the presence of the transposon in the locus involved, were purified and physically mapped with PstI and NotI, and the sequence was obtained from the junction next to the transposon to determine the gene interrupted using the SeqA and SeqB primers provided by the manufacturer.

In silico analysis of loci. Detailed analysis of the amino acid sequence of putative open reading frames (ORFs) within *mel* and *mrl* loci was carried out by using protein-protein National Center for Biotechnology Information BLAST (5) and Conserved Domain Search (64) as described previously (32).

Construction of *M. marinum* mutants by allelic exchange. In order to construct mutations in the *M. marinum mel* and *mrl* loci identified, we cloned each locus into the unique BamHI, EcoRI, or HindIII site of pYUB174 for allelic exchange as described previously (32). Each locus was in vitro mutagenized randomly using a kanamycin-resistant mini-*Mu* transposon as recommended by the manufacturer of the system (Finnzymes). Plasmids that carried mutations in genes of interest were then transformed into *M. marinum* by electroporation, and recombinants were selected for by the presence of kanamycin-resistant blue colonies on X-Gal M-ADC plates. Individual colonies were then grown in the presence of kanamycin, plated for single colonies on the same plates, and screened visually for white colonies, which should be mutants resulting from allelic exchange. The presence of the appropriate mutation was confirmed in each case by PCR and Southern analyses.

Construction of complementing strains for each *M. marinum* mutant. Complementing constructs were made for each region by high-fidelity PCR and cloning into pJDC89 as described previously (66). Basically, the fragments were amplified by PCR directly from *M. marinum* chromosomal DNA using oligonucleotides described in Table 1 and cloned directionally into pJDC89 by using NheI and PacI (pJDC117) or PacI and ScaI (pJDC119, pJDC120, and pJDC121). All constructs were confirmed by physical mapping with restriction enzymes, and the absence of mutations incorporated by PCR was demonstrated by sequencing.

Microscopic method to confirm efficiency of macrophage infection. Macrophage infection assays were conducted and evaluated by microscopy as described previously (33). Coverslips were seeded with macrophages in 24-well tissue culture plates. Bacteria were added to achieve a multiplicity of infection of 10. The infection was allowed to proceed for 30 min, after which the cells were washed twice with PBS. The cells were fixed with methanol, washed once with PBS, and stained by the Ziehl-Neelsen technique (47), using carbol-fuchsin and malachite green (Sigma). Cells were examined by using a Nikon TE300 light microscope with differential interference contrast optics. At least two independent coverslips were examined for each sample. The percentage of infected cells was determined for three counts of 25 fields, each with greater than 20 cells per field. The number of bacterial vacuoles per cell was determined for three counts of 50 cells each, and the number of bacteria per vacuole was determined for three counts of 50 cells each. These values were used to calculate an infectivity index for each mutant as the (percent infected cells \times the number of vacuoles per

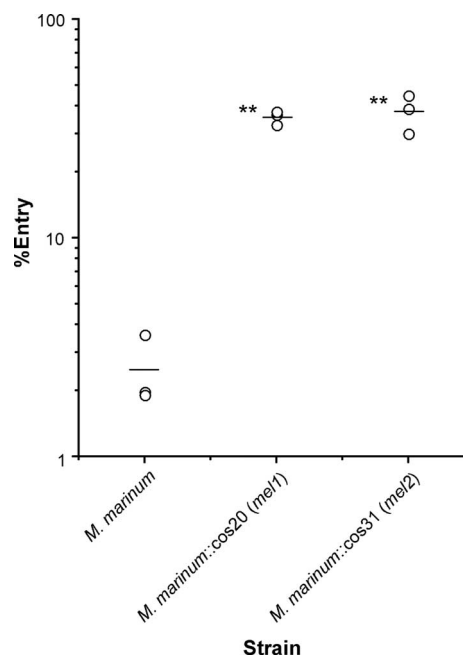


FIG. 2. Percentage of the bacterial inoculum that enters murine macrophage RAW 264.7 cells for wild-type *M. marinum* and *M. marinum* that carry cosmids that have the mycobacterial enhanced infection loci *mel1* (*M. marinum::cos20*) and *mel2* (*M. marinum::cos31*). All culture densities were approximately 0.5 at 600 nm. Each point represents the mean of triplicate samples. The line for each strain represents the mean of the three independent experiments. **, $P < 0.001$ compared to wild-type *M. marinum*.

cell \times the number of bacteria per vacuole for strain)/(percent infected cells \times the number of vacuoles per cell \times the number of bacteria per vacuole for *M. marinum*). All microscopy samples were coded to allow blinded examination.

Statistical analyses. All experiments were carried out in triplicate and repeated at least three times, except where specifically noted. The significance of the results was determined by using the Student *t* test or analysis of variance, where appropriate. P values of < 0.05 were considered significant.

RESULTS

Macrophage infection by *M. marinum* is regulated. Genes involved in the virulence of bacterial pathogens are usually tightly regulated under different environmental conditions to allow economic use of available nutritional resources (28, 67, 68, 85). We examined the ability of *M. marinum* to infect macrophages during growth in laboratory medium to better understand how the genes involved might be regulated and their mechanism of action. *M. marinum* displays approximately 10- to 20-fold-higher levels of macrophage infection at an OD_{600} of between 0.8 and 1.2 compared to early or late stages of growth (Fig. 1). This difference is consistent in human, murine, and fish monocytic cells and macrophages, although there are some differences in the magnitude of the effect seen. Since all assays, irrespective of the growth state of the bacteria, were conducted with the same number of bacteria in the same fashion, it is unlikely that this difference is due to experimental conditions other than regulation of the *M. marinum* factors involved.

Gene dosage effects allow subtle upregulation of genes in *M. marinum*. Our previous studies allowed identification of two

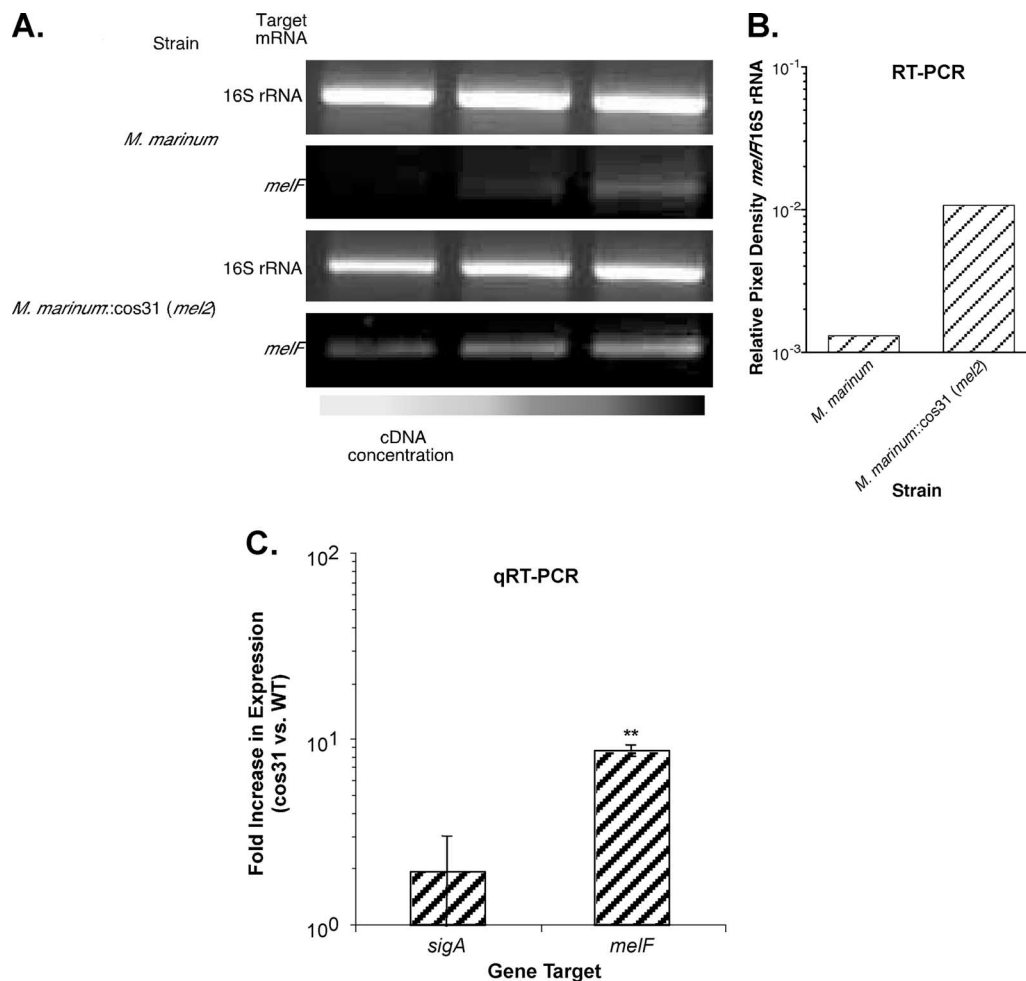


FIG. 3. RT-PCR (A and B) and quantitative RT-PCR (C) studies to evaluate the effects of gene dosage on expression of *melF* in *M. marinum*. Equivalent amounts of RNA from *M. marinum* wild-type and *M. marinum* carrying *cos31* (*M. marinum::cos31*) were reverse transcribed and subjected to PCR using specific oligonucleotides within *melF* and 16S rRNA. (A) The dilutions of cDNAs are, from left to right: 1:4, 1:2, and 1:1. Equal amounts of each PCR product were loaded on 0.8% agarose gels and compared to the 16S rRNA control RT-PCR for each strain (16S rRNA) carried out on the same samples in the same manner by ethidium bromide staining (A) and densitometry (B). (C) Quantitative RT-PCR analyses of increased expression levels of RNA transcript in *M. marinum* carrying *cos31* compared to wild-type *M. marinum* confirmed conventional RT-PCR studies. In the case of quantitative RT-PCR, the *sigA* gene was used as a control that should not display changes in expression in the presence of the cosmids. All transcript levels were calculated by the comparative C_T method using 16S rRNA as a comparator. The data shown are representative of two independent experiments. **, $P < 0.05$ compared to *sigA*.

loci, *mel1* and *mel2*, from *M. marinum* that have the ability to confer enhanced infection of macrophages to *M. smegmatis*, a nonpathogenic mycobacterial species (32). Since mutations in these loci affect the ability of *M. marinum* to infect macrophages, their regulation may be at least partially responsible for the differences in efficiency of macrophage infection observed at different stages of growth in laboratory medium. Based on these observations, we hypothesized that *M. marinum* containing plasmids that carry the *mel* loci would upregulate these genes and display enhanced macrophage infection compared to wild-type bacteria. We found that cosmids containing the *mel1* or *mel2* loci confer >10-fold-enhanced infection of macrophages to *M. marinum* (Fig. 2). When we examined the level of expression of *mel2* in wild-type *M. marinum* and the strain carrying the cosmid that contains *mel2*, we found that expression of the *melF* gene within this locus increases at least fivefold (Fig. 3). These observations suggest that gene

dosage effects can be used to increase the expression of genes involved in macrophage infection and raises the possibility that this technique could be used to identify additional macrophage infection genes.

Whole-genome screen for *M. marinum* genes involved in macrophage infection. In order to gain additional insight into the mechanisms of macrophage infection by *M. marinum*, we developed a strategy using gene dosage effects to screen the *M. marinum* genome. We first constructed a total DNA genomic cosmid library that can replicate in both *E. coli* and *M. marinum* (32). We arrayed 384 individual *E. coli* clones from this library in four 96-well plates, transformed each of these cosmids into *M. marinum*, and arrayed the resulting transformants in 96-well plates in the same manner. Since the average fragment size for the cosmid library is ~45 kbp and the *M. marinum* genome is ~6.6 Mbp, 384 clones provide ~2.6-fold coverage of the entire *M. marinum* genome or a 93% likelihood

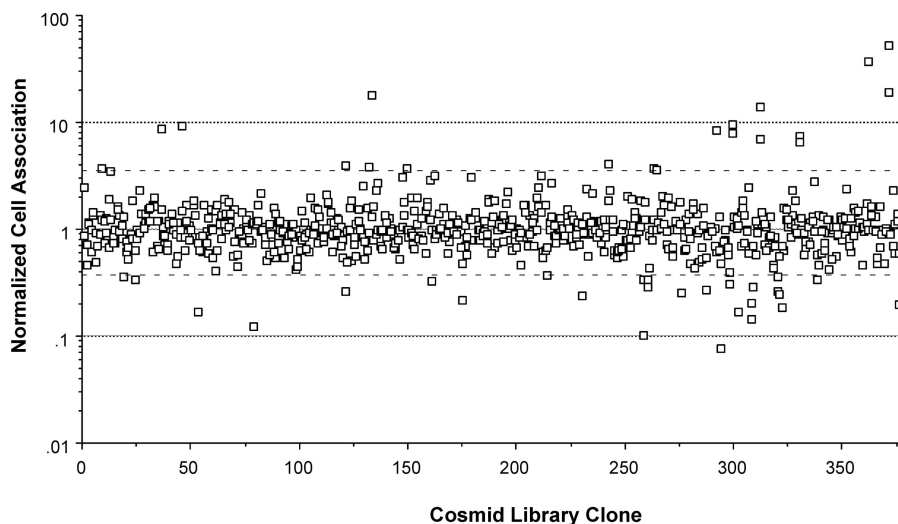


FIG. 4. Summary of all data from normalized cell association with the RAW 264.7 murine macrophage cell line for 384 individual clones of *M. marinum* carrying an arrayed *M. marinum* total genomic DNA cosmid library assayed in two independent assays in triplicate. Each data point represents the normalized mean of triplicate samples. All cell association data are normalized to the median of all library clones arbitrarily set to 1. Horizontal dashed lines indicate one standard deviation from the median, and the horizontal dotted lines indicate two standard deviations from the median.

that the entire genome is represented in the library. Each of the resulting *M. marinum* clones carrying a cosmid with a large fragment of the *M. marinum* genome was then screened in two independent assays in triplicate for the ability to infect macrophages (Fig. 4). We chose to avoid use of antibiotics in this screen to eliminate the possibility that some of the differences observed would be due to differences in antibiotic susceptibility, rather than interactions with macrophages. To normalize our data, the median level of macrophage infection for the entire library was set to 1, and results from each assay were evaluated for significant differences from the median ($P < 0.05$). Interestingly, an approximately equivalent number of clones display decreased (repressed) and increased (enhanced) macrophage infection in these assays. Since it is possible that repression of host cell infection is equally as important as enhancement of host cell infection during pathogenesis, we selected both types of clones for further analyses. A total of 76 clones had significantly enhanced or repressed macrophage infection in our initial screen.

Confirmation of the ability of cosmids to confer effects on macrophage infection. Individual cosmids that we isolated from the 76 *M. marinum* clones displaying enhanced or repressed macrophage infection were screened for similar physical maps, the presence of previously identified loci, and the ability to confer the expected phenotype when transformed back into *M. marinum*. Restriction patterns with PstI and NotI were examined for all 76 cosmids (data not shown). Four plasmids with identical restriction patterns were identified and eliminated from further analyses. In addition, we examined each cosmid for the presence of either *mel1* or *mel2* by PCR (data not shown), since these loci had been previously shown to confer enhanced macrophage infection. We identified 11 clones out of 76 that carry either *mel1* or *mel2*, and these clones were not analyzed further. Transformation of cosmids back into *M. marinum* was used to confirm their phenotype and

ensure that it is due to genes present on the cosmid, rather than a mutation in the *M. marinum* chromosome. All 76 clones resulting from transformation of these cosmids back into *M. marinum* were assayed in triplicate in three independent assays in the same manner as our initial screen (Fig. 5). We identified eight cosmid clones that confer significantly enhanced or repressed macrophage infection compared to the median for all assays ($P < 0.05$). These cosmids have unique restriction patterns and do not carry either the *mel1* or *mel2* locus. Four of these cosmids, two that confer enhanced macrophage infection (*mel*) and two that confer repressed macrophage infection (*mrl*), were chosen for further analysis.

Identification of *M. marinum mel* and *mrl* loci. Physical maps were constructed for all four cosmids, and the cosmids were in vitro mutagenized with a chloramphenicol-resistant mini-*Mu* transposon. Each cosmid displays a unique NotI physical map and ranges in size from 44 to 52 kbp (Fig. 6). The exact locations of transposon insertions in each cosmid were determined by sequencing out from the transposon. Cosmids that carried unique transposon insertions in the insert *M. marinum* DNA were transformed into *M. marinum* to evaluate whether the mutagenized cosmid retained the ability to confer the expected phenotype for macrophage infection compared to wild-type *M. marinum* and the nonmutated cosmid. These assays were carried out three times independently in triplicate, and mutagenized cosmids that display a significantly different phenotype compared to the original cosmid ($P < 0.05$) were concluded to have a transposon insertion in the locus affecting macrophage infection (Fig. 6). We identified one region from each cosmid that is involved in either enhancing, designated *mel3* and *mel4*, or repressing, designated *mrl1* and *mrl2*, macrophage infection by *M. marinum*. Based on the positions of each transposon insertion and their effect on the phenotype conferred by the cosmid, we estimated the approximate size of

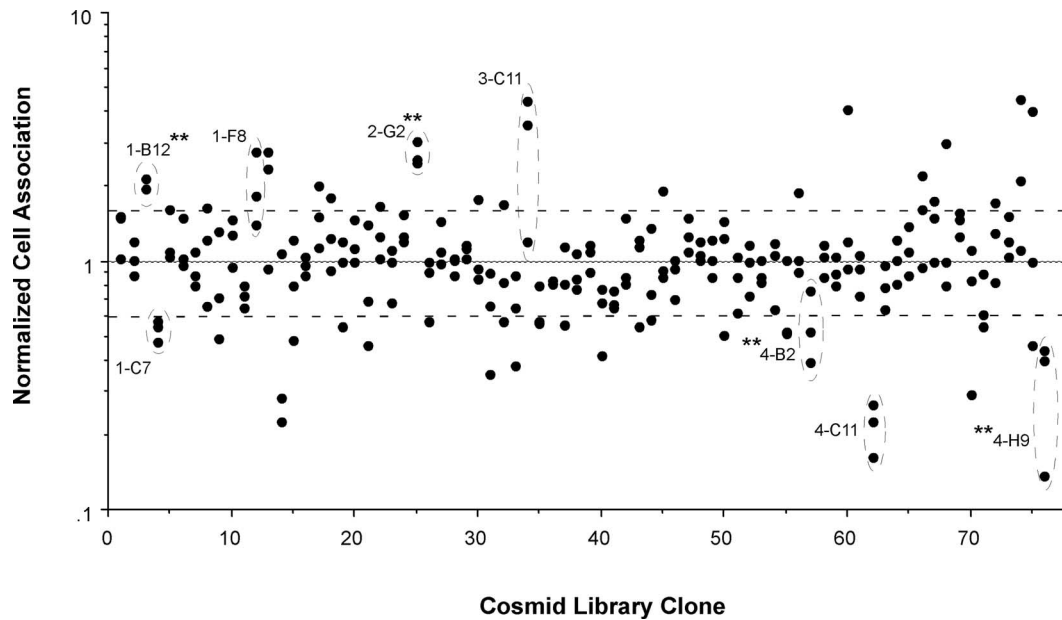


FIG. 5. Normalized cell association data in the RAW 264.7 murine macrophage cell line for 76 cosmid clones chosen from the original *M. marinum* total genomic DNA cosmid library assayed in three independent assays in triplicate. Each data point represents the normalized mean of triplicate samples. All cell association data are normalized to the mean of all library clones arbitrarily set to 1. Horizontal dashed lines indicate one standard deviation from the mean. Dashed circles indicate the eight library clones that are significantly different from the mean ($P < 0.05$), and the “**” symbols indicate the four clones chosen for further analyses.

each locus. The *mel2* and *mel3* loci are somewhat smaller (3 to 6 kbp) than the *mrl1* and *mrl2* loci (8 to 10 kbp).

In silico and expression analysis of *mel* and *mrl* loci. Sequences obtained from each transposon insertion were compared to the *M. marinum* genome available from the *M. marinum* Sequencing Group at the Sanger Institute (http://www.sanger.ac.uk/Projects/M_marinum/). This allowed determination of the complete sequence of each locus and annotation of the regions involved (Fig. 7). Quantitative RT-PCR analyses of the transcript levels of the genes identified within the *mel4* and *mrl2* loci confirm that the cosmids 2-G2 and 4-H9 increase

expression of the loci that they carry when present in *M. marinum* (Fig. 7), similar to our observations with the cosmid that carries *melF*. The loci identified are not clustered in an obvious fashion in the *M. marinum* genome and are unique with respect to previously identified *M. marinum* virulence determinants. We analyzed the putative coding regions within these loci for similarity to other bacterial genes and motifs present within them to gain insight into their potential functions. Detailed in silico analysis of the putative ORFs identified in this manner is described in Table 2. Based on these analyses, the *mel3* locus carries a single ORF that is similar to the mycobacterial PknD,

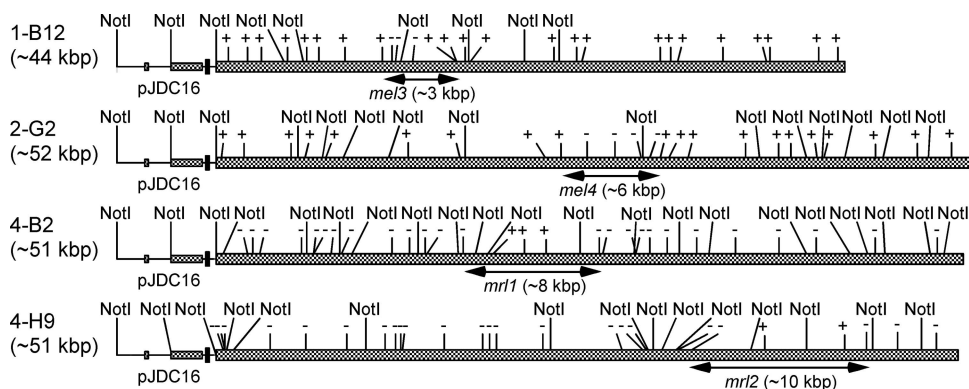


FIG. 6. Physical maps (NotI) of four cosmids, 1-B12, 2-G2, 4-B2, and 4-H9, that affect cell association of *M. marinum*, approximate total plasmid and locus size (in parentheses), the positions of transposon insertions, and the phenotype of insertion. Plus markers indicate that the cosmid carrying a transposon insertion at that location enhances host cell infection, and minus markers indicate that insertion represses host cell infection. Loci identified by transposon mutagenesis were designated *mel* for “mycobacterial enhanced infection locus” or *mrl* for “mycobacterial repressed infection locus” based upon the phenotype that the original cosmid confers to wild-type *M. marinum*. All cosmids carrying transposon insertions were assayed for cell association with the RAW 264.7 murine macrophage cell line three times independently in triplicate to determine the phenotypic effects that they confer compared to the original cosmid.

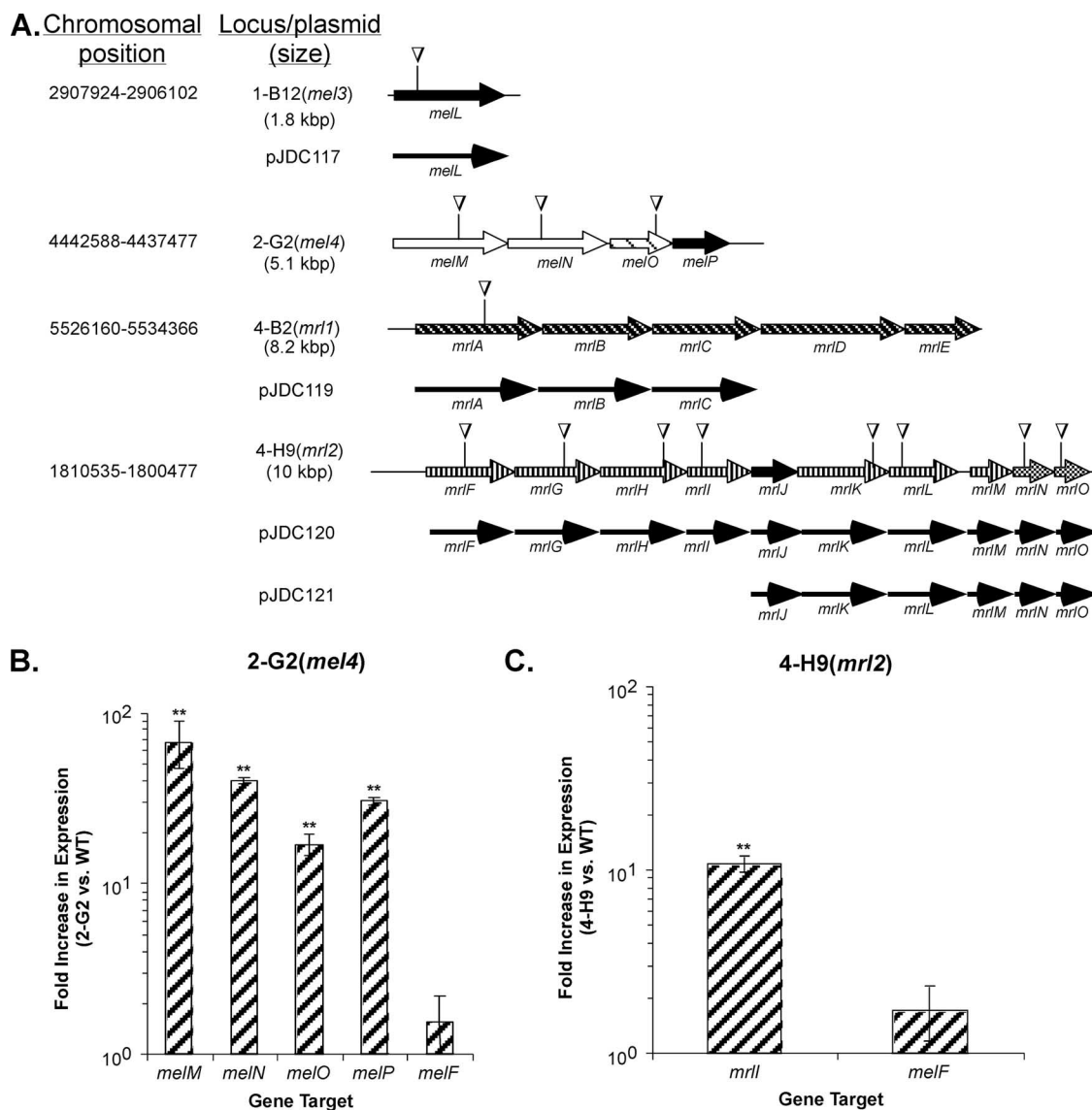


FIG. 7. (A) Position of each *mel* and *mrl* locus on the *M. marinum* chromosome as obtained from the *M. marinum* Sequencing Group at the Sanger Institute (http://www.sanger.ac.uk/Projects/M_marinum/), size of each locus, deduced gene map of each locus, and structure of regions used in complementation plasmids. Triangles indicate positions of insertion mutations used to construct *M. marinum* mutants in each locus by allelic exchange. (B and C) Quantitative RT-PCR analyses for levels of RNA transcript in wild-type *M. marinum* and *M. marinum* carrying cosmids (2-G2 for *mel4* and 4-H9 for *mrl2*) for *melM-P* genes in the *mel4* locus (B) and the *mrlI* gene in the *mrl2* locus (C). The *melF* gene was used as a control that should not display changes in expression in the presence of these cosmids. All transcript levels were calculated by the comparative C_T method using 16S rRNA as a comparator. The data shown are the means and standard deviations for two independent experiments carried out in triplicate. **, significantly different fold increase in expression compared to the *melF* gene under the same conditions ($P < 0.05$).

a “eukaryotic-like” serine/threonine kinase that appears to affect regulation through SigF (42, 44, 80). The *mel4* locus encodes four putative ORFs, two of which are similar to zinc-dependent proteases and two with unknown functions. Interestingly, both of the *mrl* loci identified contain ORFs with potential involvement in synthesis of the mycobacterial cell wall. There are five putative ORFs within *mrl1* that display similarity to cell wall biosynthetic proteins in other bacteria and ten putative ORFs within *mrl2* that primarily display similarity to lipid biosynthetic proteins. Since lipids are an important component of the mycobacterial cell wall, it is possible that *mrl1* and *mrl2* are involved in synthesis of modified my-

cobacterial cell wall components, resulting in a composition that is less conducive to efficient phagocytosis by macrophages under certain growth conditions.

Mutations in *M. marinum* *mel* loci affect infection of macrophages. To eliminate the possibility that the phenotypes conferred by *mel* and *mrl* loci are due to artifacts resulting from overexpression, rather than the natural gene functions, we constructed mutations in them by allelic exchange and examined their effects on macrophage infection. Each locus was first cloned into a suicide plasmid for mycobacteria, pYUB174, and mutated by in vitro transposon mutagenesis. The exact location of each transposon insertion was determined by sequencing

TABLE 2. Characteristics of genes in *mel* and *mrl* loci

Gene locus	Similar organism (gene) ^a	E value (score) ^b	% Identity (no. of aa) ^c	Other similarities or motifs ^d	Putative activity
<i>mel3</i>					
<i>melL</i>	<i>M. smegmatis</i> (<i>pknD</i>)	3e-94 (349)	66 (272)	S_TKc, DUF477	Serine/threonine kinase
<i>mel4</i>					
<i>melM</i>	<i>M. tuberculosis</i> (Rv2315c)	0.0 (859)	86 (505)	COG0312, Zn-dep.prot.	Protease
<i>melN</i>	<i>M. tuberculosis</i> (Rv2314c)	0.0 (711)	84 (457)	COG0312, Zn-dep.prot.	Protease
<i>melO</i>	<i>M. tuberculosis</i> (Rv2313)	5e-113 (410)	84 (283)	COG2128, unchar.cons.prot.	Unknown
<i>melP</i>	<i>N. farcinica</i> (<i>nfa42450</i>)	3e-13 (78.6)	52 (91)	None	Unknown
<i>mrl1</i>					
<i>mrlA</i>	<i>Arthrobacter</i> sp. (Arth4051)	2e-47 (194)	46 (276)	COG1922, teich.ac.syn.	Cell wall biogenesis
<i>mrlB</i>	<i>M. avium</i> subsp. <i>paratuberculosis</i> (MAP0964c)	0.0 (704)	71 (507)	COG2148, sug.trans.lps, COG1086, nuc.diph.ep.	Cell wall biogenesis
<i>mrlC</i>	<i>M. avium</i> subsp. <i>paratuberculosis</i> (MAP0963c)	3e-150 (535)	68 (488)	pfam01943, polys.syn., COG0728, MviN	Cell wall biogenesis
<i>mrlD</i>	<i>M. avium</i> subsp. <i>paratuberculosis</i> (MAP0962c)	0.0 (685)	63 (663)	COG1216, glyc.tran., pfam00534, glyc.tran1	Cell wall biogenesis
<i>mrlE</i>	<i>M. avium</i> subsp. <i>paratuberculosis</i> (MAP0961c)	8e-125 (449)	72 (349)	COG0438, glyc.tran.	Cell wall biogenesis
<i>mrl2</i>					
<i>mrlF</i>	<i>M. avium</i> subsp. <i>paratuberculosis</i> (MAP3191)	0.0 (646)	87 (370)	pfam04209, hom.diox.	Phe and Tyr metabolism
<i>mrlG</i>	<i>M. avium</i> subsp. <i>paratuberculosis</i> (MAP3192)	0.0 (711)	87 (392)	COG1506, dip.amin.pep.	Amino acid transport/metabolism
<i>mrlH</i>	<i>M. avium</i> subsp. <i>paratuberculosis</i> (MAP3193)	0.0 (685)	90 (396)	COG1804, acCoA-trans.	Lipid transport/metabolism
<i>mrlI</i>	<i>M. avium</i> subsp. <i>paratuberculosis</i> (MAP3194)	2e-104 (381)	81 (301)	pfam00682, aldolase	Metabolism
<i>mrlJ</i>	<i>M. avium</i> subsp. <i>paratuberculosis</i> (MAP3195)	1e-87 (325)	80 (213)	pfam00440, TetR_N, COG1309, AcrR	Transcriptional regulation
<i>mrlK</i>	<i>M. avium</i> subsp. <i>paratuberculosis</i> (FadE12-3)	0.0 (734)	87 (412)	cd00567, ACAD	Lipid metabolism
<i>mrlL</i>	<i>M. avium</i> subsp. <i>paratuberculosis</i> (MAP3197)	3e-89 (322)	75 (264)	COG1960, ACAD pfam01636, phosphotr.	Metabolism
<i>mrlM</i>	<i>M. avium</i> subsp. <i>paratuberculosis</i> (MAP3198)	5e-37 (156)	62 (129)	COG3631, ketost.isom.	Metabolism
<i>mrlN</i>	<i>M. avium</i> subsp. <i>paratuberculosis</i> (MAP3199)	2e-56 (221)	64 (173)	pfam04264, YceI	Unknown
<i>mrlO</i>	<i>M. tuberculosis</i> (Rv3143)	7e-55 (216)	88 (130)	Cd00156, sig.rec.	Signal receiver

^a That is, the organism that carries the protein most similar to that encoded by the *M. marinum* gene identified, along with the name of the corresponding gene in that organism in parentheses.

^b The expectation frequency (E value) is a parameter that describes the significance of the sequence match and the score of the sequence match according to NCBI protein-protein BLAST when it is compared to the closest homologue.

^c The percent identity at the amino acid (aa) level and the number of amino acids (in parentheses) that could be aligned to show this level of identity.

^d This column indicates the placement of the putative protein product into a cluster of orthologues (COG or KOG [eukaryotic]) using the CD-Search at NCBI and SignalP v.1.1 at the Center for Biological Sequence Analysis website. COG, clusters of orthologous groups; KOG, clusters of orthologous groups for eukaryotic genomes; pfam, protein family; cd, conserved domain; S_TKc, serine/threonine protein kinase catalytic domain; DUF477, domain of unknown function found in *Eukarya* and *Eubacteria*; Zn-dep.prot., Zn-dependent proteases; unchar.cons.prot., uncharacterized conserved protein; teich.ac.syn., teichoic acid synthesis proteins; sug.trans.lps, sugar transferases involved in lipopolysaccharide synthesis; nuc.diph.ep., predicted nucleoside-diphosphate sugar epimerase; polys.syn., polysaccharide biosynthesis protein; MviN, uncharacterized membrane protein thought to be involved in virulence; glyc.tran., predicted glycosyltransferases; glyc.tran1, glycosyl transferases group 1; hom.diox., homogentisate 1,2-dioxygenase involved in the metabolism of Phe and Tyr; dip.amin.pep., dipeptidyl aminopeptidases/acylaminoacyl-peptidases; TetR_N, TetR family bacterial regulatory proteins; AcrR, AcrR family of transcriptional regulators; ACAD, acyl-coenzyme A dehydrogenase; phosphotr., phosphotransferase enzyme family; ketost.isom., ketosteroid isomerase; YceI, *E. coli* YceI-like family of inducible periplasmic proteins; sig.rec., signal receiver domain.

from the transposon. We identified insertions in *melL*, *melM*, *melN*, *melO*, *mrlA*, *mrlF*, *mrlG*, *mrlH*, *mrlI*, *mrlK*, *mrlL*, *mrlN*, and *mrlO* using this technique (Fig. 7). Each of these mutations was then transferred to *M. marinum* by allelic exchange using the β -galactosidase gene carried by this pYUB174 to screen for single and double recombination events in a two-step allelic exchange. Each of the resulting mutants was compared for its ability to infect macrophages with wild-type *M. marinum* and *M. marinum* carrying the original cosmid (Fig. 8). As expected, the *melL* mutant displays a significant defect ($P < 0.01$) in

macrophage infection compared to wild-type *M. marinum*. Although transposon insertions in these genes within the original *mel4* cosmid affect the ability of the cosmid to enhance macrophage infection, *melM*, *melN*, and *melO* mutants do not display a significant defect in macrophage infection and may actually display enhanced macrophage infection. We hypothesized that the functional ORF within the *mel4* locus might be *melP*, rather than the other three genes. Since we did not obtain a mutation in this gene, we could not test the role of *melP* directly, but we examined whether its transcription was

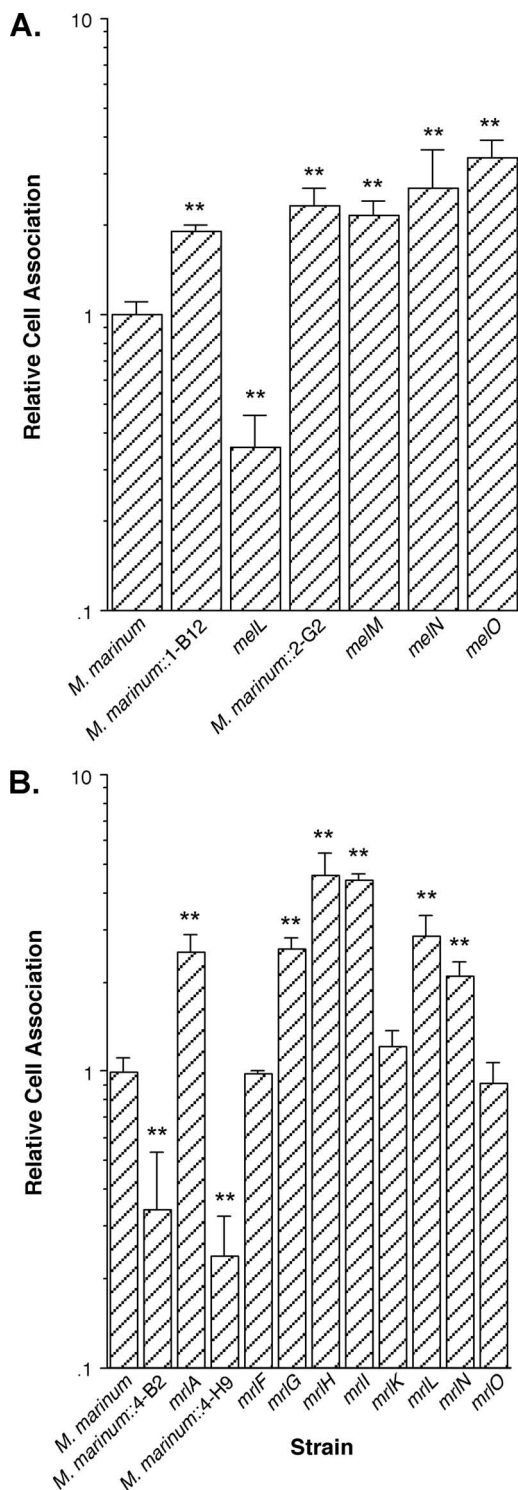


FIG. 8. Cell association of *M. marinum* wild type, *M. marinum* mutants, and *M. marinum* containing cosmid 1-B12 that carries *melL*, 2-G2 that carries *melMNOP*, 4-B2 that carries *mrlABCDE*, and 4-H9 that carries *mrlFGHIJKLMNO* with RAW 264.7 cells. The data are expressed relative to the cell association of wild-type *M. marinum* that was included as an internal control in all experiments. The data and error bars represent the means and standard deviations, respectively, of three independent experiments carried out in triplicate. **, $P < 0.05$ compared to wild-type *M. marinum*.

affected by the insertions in the other ORFs within *mel4* (Fig. 9). We found that insertions in each of the *mel4* ORFs affected all genes downstream, with the exception of *melP*, suggesting that the *melP* gene is within a different transcriptional unit from the other genes within *mel4*. The phenotype of mutants that affect macrophage infection was confirmed by microscopy using acid-fast stains (Table 3). Acid-fast stains revealed similar differences in the ability of these mutants and the original cosmids to infect macrophages, as observed in cell association assays. Since both viability-based assays, such as cell association assays, and microscopy, which is not affected by bacterial viability, display similar results, it is unlikely that survival in host cells is solely responsible for their phenotype. Rather, the observed phenotype is most likely due to differences in macrophage infection.

Mutations within *mrl* loci enhance macrophage infection. Since the presence of the *mrl* loci on cosmids represses infection of macrophages, most likely due to gene dosage effects, we expected that mutants in these genes could enhance macrophage infection. We found that *M. marinum mrlA*, *mrlG*, *mrlH*, *mrlI*, *mrlL*, and *mrlN* mutants display enhanced macrophage infection compared to the wild type ($P < 0.01$), whereas *mrlF*, *mrlK*, and *mrlO* mutants infect macrophages at levels similar to the wild type (Fig. 8). These observations suggest that *mrlF* and *mrlO* are not required for inhibition of macrophage infection. This may be the case for *mrlK* as well, although this mutation might not interfere with the activity of the protein product due to its carboxy-terminal position of insertion. However, the other predicted *mrl* genes—*mrlA*, *mrlG*, *mrlH*, *mrlI*, *mrlL*, and *mrlN*—play a role in reducing macrophage infection by wild-type *M. marinum*.

Complementation restores wild-type macrophage infection to *mel* and *mrl* mutants. In order to ensure that secondary mutations had not occurred elsewhere in the *M. marinum* chromosome during mutagenesis of the *mel* and *mrl* loci, we transformed each mutant with a plasmid carrying the appropriate wild-type chromosomal regions. The mutant, wild-type and complementing strains were then compared for their ability to infect macrophages, and we found that complementation restores the expected phenotype (Fig. 10). The *mrlA* mutation could be complemented with the *mrlA* through *mrlC* region alone, so we suspect that either *mrlD* and *mrlE* are in a different transcriptional unit or they are not required for reduction of macrophage infection. The *mrlI* mutation could be complemented by the entire *mrl2* locus but not the *mrlI* through *mrlO* region alone, confirming the importance of *mrlI* for reduction of macrophage infection. These data suggest that the genes within the *mel* and *mrl* loci are responsible for the effects of each cosmid on macrophage infection by *M. marinum* and that gene dosage effects allowed identification of novel genes that are involved in interactions with macrophages by wild-type *M. marinum*.

DISCUSSION

Macrophage infection by bacteria involves a complex interplay between adherence, phagocytosis, and initial intracellular survival. Since mycobacteria are thought to replicate primarily within macrophages during disease, it is likely that proper interactions with macrophages are critical to pathogenesis. In-

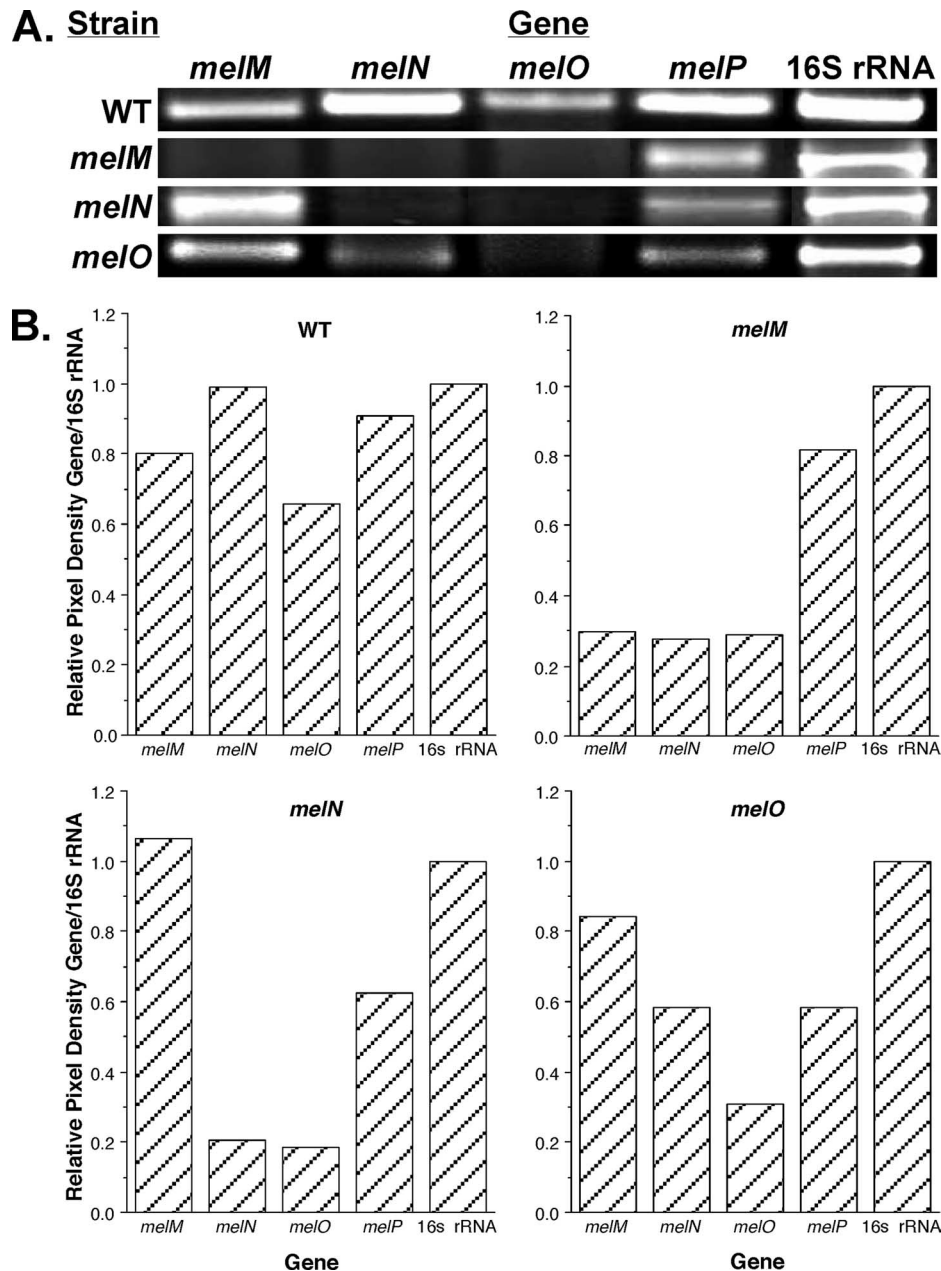


FIG. 9. RT-PCR studies to evaluate the effects of insertion mutations on expression of *melM*, *melN*, *melO*, and *melP* in *M. marinum*. Approximately equivalent amounts of RNA from *M. marinum* wild-type and *M. marinum melM*, *melN*, *melO*, and *melP* mutants were reverse transcribed and subjected to RT-PCR with specific oligonucleotides within *melM*, *melN*, *melO*, and *melP* and 16S rRNA. Equal amounts of each PCR product were loaded on 0.8% agarose gels and compared to the 16S rRNA control RT-PCR for each strain (16S rRNA) carried out on the same samples in the same manner by ethidium bromide staining (A) and densitometry (B). The data shown are representative of two independent experiments where similar results were obtained in both.

fection of macrophages by *M. marinum* is dependent upon the stage of growth in laboratory medium, suggesting that the genes involved in macrophage infection are regulated. This observation, combined with the ability of gene dosage to increase the expression of genes, was utilized in the present study to identify *M. marinum* genes involved in macrophage infection. This approach is advantageous because it allows the entire genome to be screened using relatively few clones, since cosmids can contain a large numbers of genes. The conclusion

that this approach allowed identification of genes involved in the normal interactions of wild-type *M. marinum* with macrophages is supported by the fact that specific mutants in these genes display the expected phenotype and complementation results in recovery of the wild-type phenotype. In addition, the phenotype of each cosmid and mutant was confirmed by microscopy, which suggests that the effect is on macrophage infection rather than on survival either within the cells or during the experimental procedure. Furthermore, studies in *Salmo-*

TABLE 3. Infection of murine macrophages

Strain	Mean \pm SD			
	% Infected cells ^a	No. of vacuoles/cell ^b	No. of bacteria/vacuole ^c	Infectivity index ^d
<i>M. marinum</i>	14 \pm 1.0	1.2 \pm 0.6	10 \pm 7.8	1.0 \pm 0.10
<i>M. marinum</i> ::1-B12	51 \pm 4.7	2.1 \pm 1.3	15 \pm 9.8	9.6 \pm 0.77*
<i>M. marinum</i> (<i>melL</i>)	3.7 \pm 0.9	1.1 \pm 0.2	9.5 \pm 6.8	0.2 \pm 0.05*
<i>M. marinum</i> ::2-G2	49 \pm 5.2	2.1 \pm 1.6	12 \pm 8.3	7.4 \pm 0.79*
<i>M. marinum</i> ::4-B2	6.1 \pm 2.3	1.0 \pm 0.4	16 \pm 13	0.6 \pm 0.23†
<i>M. marinum</i> (<i>mrlA</i>)	30 \pm 5.3	2.2 \pm 1.3	11 \pm 6.0	4.3 \pm 0.76*
<i>M. marinum</i> ::4-H9	7.2 \pm 1.1	1.1 \pm 0.3	13 \pm 9.1	0.6 \pm 0.09*
<i>M. marinum</i> (<i>mrlG</i>)	37 \pm 2.1	1.9 \pm 1.4	11 \pm 8.3	4.6 \pm 0.06*
<i>M. marinum</i> (<i>mrlL</i>)	28 \pm 2.5	1.1 \pm 0.6	14 \pm 12	2.6 \pm 0.23*

^a That is, the percentage of cells containing at least one bacterium in a field. The results are the means \pm standard deviations for three counts of 25 fields.

^b That is, the number of bacterial vacuoles in each cell. Results are the means for three counts of 50 cells.

^c That is, the number of bacteria in each vacuole. Results are means \pm the standard deviations for three counts of 50 cells.

^d The infectivity index was calculated as follows: (% infected cells \times the number of vacuoles per cell \times the number of bacteria per vacuole for the strain)/(% infected cells \times the number of vacuoles per cell \times the number of bacteria per vacuole for *M. marinum*). *, Significantly different from wild type *M. marinum* ($P < 0.01$); †, significantly different from wild-type *M. marinum* ($P < 0.05$).

nella (54) and *Legionella* (17, 85) strains have yielded similarly promising results using comparable strategies to increase expression of virulence genes to allow their identification by functional assays.

Gene dosage has been used previously to control regulation of genes of interest (2, 8, 77) and has been used successfully by our own group for whole-genome screens for virulence genes in *Legionella* (17). One caveat of this approach could be that operator regions present on the cosmids might saturate regulators, resulting in down- or upregulation of unlinked loci in the same regulon (50, 53, 77). We have not previously found unlinked loci that were responsible for the observed phenotype, nor was this type of problem observed in the present study, since mutations in the loci identified display the expected phenotype. This problem may have been avoided because our studies have utilized relatively low-copy-number vectors. The mycobacterial origin of replication on our cosmid is derived from pAL5000, thought to be a low-copy-number plasmid (94). This fact most likely allowed relatively subtle enhancement of the expression of genes that this plasmid carries in our library, rather than extremely robust expression that might be detrimental to bacterial growth in vitro and lead to pleiotropic effects. The conclusion that this library only results in subtle increases in expression is supported by our observation that the presence of a cosmid containing *mel2* in *M. marinum* increases the expression of *melF* approximately 5- to 10-fold. This level of expression allowed identification of loci that are involved in macrophage infection in wild-type *M. marinum*, rather than only affecting macrophage infection when overexpressed. These observations suggest that we are examining the natural function of these genes, rather than an indirect effect of overexpressing them.

Our initial screen identified 76 cosmids that had the ability to confer enhanced or repressed macrophage infection to *M. marinum*. Some of these were false positives, either because the cosmid did not confer the expected phenotype after transformation back into *M. marinum* or because they did not consistently display the same phenotype. A possible reason that some of the original cosmids did not confer the expected phenotype when transformed back into *M. marinum* is that a secondary mutation occurred in the bacterial chromosome,

which cannot be transferred. However, it is equally possible that mutations or rearrangements occur in the cosmids themselves as they are passaged back through *E. coli*. This possibility could be examined by going back to the original cosmid clones in *E. coli* and comparing them to those from *M. marinum*. Cosmids that did not display a consistent phenotype may do so because they are impacted greatly by the phase of growth of the culture or their phenotype in macrophages is less obvious under laboratory conditions. Neither issue makes the genes that they carry of less interest, although it is equally possible that they are true negatives. The only clones that we carried through our entire analysis in the present study were those that display the expected phenotype in all assays, making it possible that not all genes that could affect macrophage infection have been identified, as yet. Further studies to evaluate such clones in additional assays are ongoing and may result in the identification of additional *mel* and *mrl* loci.

Most of the *M. marinum mel* and *mrl* mutants constructed had the expected phenotype, but some mutants did not display a difference in macrophage infection compared to the wild type. Mutations in the *melM*, *melN*, and *melO* genes do not affect macrophage infection, although mutations in this locus on the cosmid affect the enhancement of macrophage infection. Although this observation could be the result of genetic buffering or redundancy (46), the absence of an effect of these mutations on *melP* expression could also explain these observations. It appears that *melP* is expressed from a different RNA transcript, despite the close proximity to *melO*. These observations might suggest that *melP* is important for the enhanced macrophage infection phenotype conferred by cosmid 2-G2. However, it is possible that the *melM-O* genes are also involved, explaining their apparent impact on macrophage infection when present on the cosmid, although it is clear that they are not individually necessary for the function of *melP* in macrophage infection. If the prediction of protease activity for *MelM* and *MelN* is correct, other proteases might compensate for a mutation in a single protease, providing functional redundancy. In fact, *MelN* may compensate for *MelM* and vice versa. Construction of a double mutant or deletion of both genes would provide some of the reagents necessary to test this possibility. More detailed analysis of this region is needed to

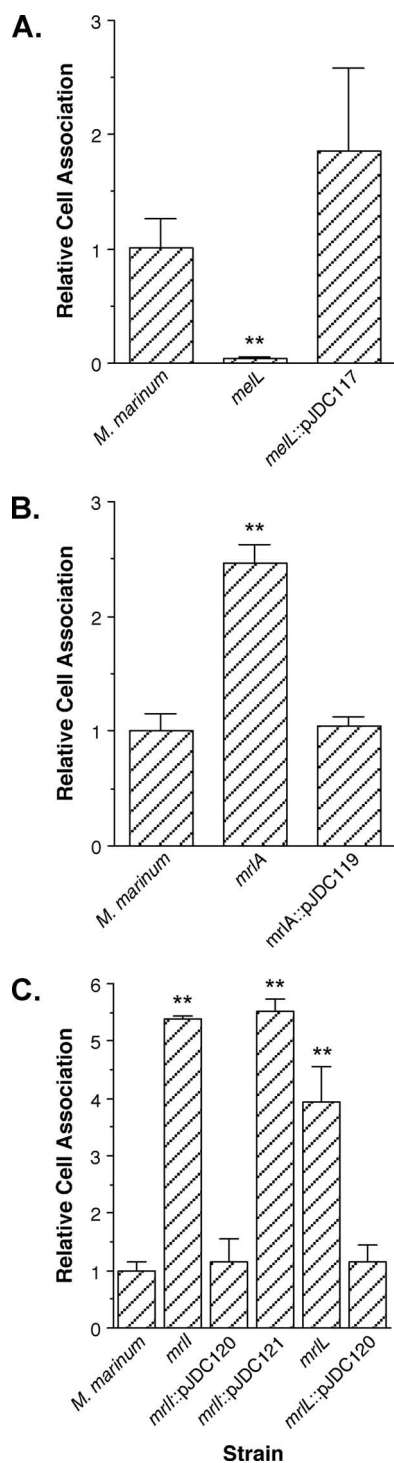


FIG. 10. Cell association of *M. marinum* wild type, *M. marinum* mutants, and mutants carrying complementing constructs with RAW 264.7 cells. All data are expressed relative to the cell association of wild-type *M. marinum* that was included as an internal control in all experiments. The data and error bars represent the means and standard deviations, respectively, of three independent experiments carried out in triplicate. **, $P < 0.01$ compared to wild-type *M. marinum*.

better understand the interactions of MelM-O with MelP, particularly because our bioinformatic analyses provided little information regarding the predicted functions of these genes.

Mutations in three of the genes—*mrlF*, *mrlK*, and *mrlL*—within *mrl2* did not affect macrophage infection. These observations may be for reasons similar to those for the *melM-O* genes. However, since two of these genes are on the periphery of the locus, these analyses may have simply allowed a more refined definition of the functional locus. The need for the entire region, rather than just the *mrlI-O* region, to complement a *mrlI* mutation suggest that at least *mrlI* is required for repression of macrophage infection. In the case of *mrlK*, the mutant may not display a phenotype due to the production of a functional protein product, since the mutation is very near the predicted carboxy terminus. Thus, we cannot, at this point, rule out a role for *mrlK* in macrophage infection, and the entire region from *mrlG* to *mrlN* may be involved. Construction of additional mutations and complementing constructs, as well as more detailed analysis of the biochemical activities of the product of each gene, should improve our understanding of the role of this locus in macrophage infection.

Interestingly, we identified cosmid clones, now designated *mrl* for “mycobacterial repressed macrophage infection loci,” that consistently confer repressed macrophage infection to *M. marinum*. This observation may be due to increased expression of repressors that control macrophage infection or genes that are involved in antiphagocytic activities. Antiphagocytic activity is often attributed to capsule on pathogenic organisms (4, 10, 25, 31, 39, 48, 58, 60, 90, 91, 105), which fits well with the predicted role of the *mrl* genes in cell wall and lipid biosynthetic pathways. Since tuberculosis and other mycobacteria can produce capsule (34, 55, 75, 76, 87, 93), it is tempting to speculate that these genes are involved in the synthesis of a capsule-like structure during certain stages of infection. However, it is equally likely that modification to the mycobacterial cell wall can modulate phagocytosis similar to the cell wall of *M. leprae* (70–72). Since mycobacteria are normally considered intracellular pathogens, the fact that there are stages of mycobacterial infection where the bacteria are primarily found extracellular (26, 56, 61, 99, 100) and may be expressing antiphagocytic activities is only rarely examined. Examples of stages where extracellular bacteria are found during tuberculosis include within liquefied lesions, on the periphery of hypoxic lesions, and possibly during dissemination (21, 22, 26, 56, 59, 61, 62). Environmental mycobacteria are likely to require the ability to persist extracellularly for an extended period of time, particularly in water environments where nutrients are usually dilute and protozoa that allow intracellular growth (15, 45, 51, 52) may be sparse (40, 43, 63, 102–104). Therefore, it seems likely that the ability to express an antiphagocytic activity at specific stages of disease would provide an advantage for pathogenic and environmental mycobacteria. These observations emphasize the importance of further studies to better understand the importance of the genes we have identified during pathogenesis.

These observations, along with our earlier studies designed to elucidate the mechanisms used by *M. marinum* to control infection of macrophages (32, 66), suggest that interactions of *M. marinum* with macrophages are complex and multifaceted. Although it seems likely that we do not yet have a comprehen-

sive picture of how *M. marinum* parasitizes macrophages, we did recover the *mel1* and *mel2* loci previously identified (32), confirming that these loci are important for interactions with macrophages and that our screen was relatively comprehensive. Four additional cosmids, beyond those characterized here in detail, were identified that display unique restriction maps and do not carry previously recognized macrophage infection loci. Studies are ongoing to better characterize these cosmids, which should provide additional insight into the molecular mechanisms of macrophage infection and may identify overlap with our earlier screen by transposon mutagenesis (66). Continued analysis of the molecular mechanisms of action of these macrophage infection loci should provide us with a much better understanding of this complex, but critical, aspect of mycobacterial pathogenesis.

ACKNOWLEDGMENT

This study was supported by grant AI47866 from the National Institutes of Health.

REFERENCES

- Abdallah, A. M., T. Verboom, F. Hannes, M. Safi, M. Strong, D. Eisenberg, R. J. Musters, C. M. Vandenbroucke-Grauls, B. J. Appelmeij, J. Luirink, and W. Bitter. 2006. A specific secretion system mediates PPE41 transport in pathogenic mycobacteria. *Mol. Microbiol.* **62**:667–679.
- Aiba, S., H. Tsunekawa, and T. Imanaka. 1982. New approach to tryptophan production by *Escherichia coli*: genetic manipulation of composite plasmids in vitro. *Appl. Environ. Microbiol.* **43**:289–297.
- Alexander, D. C., J. R. Jones, T. Tan, J. M. Chen, and J. Liu. 2004. PimF, a mannosyltransferase of mycobacteria, is involved in the biosynthesis of phosphatidylinositol mannosides and lipoarabinomannan. *J. Biol. Chem.* **279**:18824–18833.
- Almeida, R. A., and S. P. Oliver. 1993. Antiphagocytic effect of the capsule of *Streptococcus uberis*. *Zentralbl. Veterinarmed. B* **40**:707–714.
- Altschul, S. F., T. L. Madden, A. A. Schäffer, J. Zhang, Z. Zhang, W. Miller, and D. J. Lipman. 1997. Gapped BLAST and PSI-BLAST: a new generation of protein database search programs. *Nucleic Acids Res.* **25**:3389–3402.
- Barker, L. P., D. M. Brooks, and P. L. Small. 1998. The identification of *Mycobacterium marinum* genes differentially expressed in macrophage phagosomes using promoter fusions to green fluorescent protein. *Mol. Microbiol.* **29**:1167–1177.
- Barker, L. P., K. M. George, S. Falkow, and P. L. C. Small. 1997. Differential trafficking of live and dead *Mycobacterium marinum* organisms in macrophages. *Infect. Immun.* **65**:1497–1504.
- Blanc-Potard, A. B., N. Figueroa-Bossi, and L. Bossi. 1999. Histidine operon deattenuation in *dnaA* mutants of *Salmonella typhimurium* correlates with a decrease in the gene dosage ratio between tRNA(His) and histidine biosynthetic loci. *J. Bacteriol.* **181**:2938–2941.
- Bookout, A. L., C. L. Cummins, D. J. Mangelsdorf, J. M. Pesola, and M. F. Kramer. 2006. High-throughput real-time quantitative reverse transcription PCR. *Curr. Protoc. Mol. Biol.* **15**:15–18.
- Bose, I., A. J. Reese, J. J. Ory, G. Janbon, and T. L. Doering. 2003. A yeast under cover: the capsule of *Cryptococcus neoformans*. *Eukaryot. Cell* **2**:655–663.
- Broussard, G. W., and D. G. Ennis. 2007. *Mycobacterium marinum* produces long-term chronic infections in medaka: a new animal model for studying human tuberculosis. *Comp. Biochem. Physiol. C Toxicol. Pharmacol.* **145**:45–54.
- Cirillo, J. D. 1999. Exploring a novel perspective on pathogenic relationships. *Trends Microbiol.* **7**:96–98.
- Cirillo, J. D., S. L. G. Cirillo, L. Yan, L. E. Bermudez, S. Falkow, and L. S. Tompkins. 1999. Intracellular growth in *Acanthamoeba castellanii* affects monocyte entry mechanisms and enhances virulence of *Legionella pneumophila*. *Infect. Immun.* **67**:4427–4434.
- Cirillo, J. D., S. Falkow, and L. S. Tompkins. 1994. Growth of *Legionella pneumophila* in *Acanthamoeba castellanii* enhances invasion. *Infect. Immun.* **62**:3254–3261.
- Cirillo, J. D., S. Falkow, L. S. Tompkins, and L. E. Bermudez. 1997. Interaction of *Mycobacterium avium* with environmental amoebae enhances virulence. *Infect. Immun.* **65**:3759–3767.
- Cirillo, J. D., T. R. Weisbrod, and W. R. Jacobs, Jr. 1993. Efficient electrotransformation of *Mycobacterium smegmatis*. *Bio-Rad US/EG Bull.* **1360**: 1–4.
- Cirillo, S. L. G., J. Lum, and J. D. Cirillo. 2000. Identification of novel loci involved in entry by *Legionella pneumophila*. *Microbiology* **146**:1345–1359.
- Clark, H. F., and C. C. Shepard. 1963. Effect of environmental temperatures on infection with *Mycobacterium marinum* (Balnei) of mice and a number of poikilothermic species. *J. Bacteriol.* **86**:1057–1069.
- Collins, C. H., J. M. Grange, W. C. Noble, and M. D. Yates. 1985. *Mycobacterium marinum* infections in man. *J. Hyg.* **94**:135–149.
- Collins, F. M., V. Montalbino, and N. E. Morrison. 1975. Growth and immunogenicity of photochromogenic strains of mycobacteria in the footpads of normal mice. *Infect. Immun.* **11**:1079–1087.
- Converse, P. J., A. M. Dannenberg, Jr., J. E. Estep, K. Sugisaki, Y. Abe, B. H. Schofield, and M. L. Pitt. 1996. Cavitory tuberculosis produced in rabbits by aerosolized virulent tubercle bacilli. *Infect. Immun.* **64**:4776–4787.
- Converse, P. J., A. M. Dannenberg, Jr., T. Shigenaga, D. N. McMurray, S. W. Phalen, J. L. Stanford, G. A. Rook, T. Koru-Sengul, H. Abbey, J. E. Estep, and M. L. Pitt. 1998. Pulmonary bovine-type tuberculosis in rabbits: bacillary virulence, inhaled dose effects, tuberculin sensitivity, and *Mycobacterium vaccae* immunotherapy. *Clin. Diagn. Lab. Immunol.* **5**:871–881.
- Cosma, C. L., O. Humbert, and L. Ramakrishnan. 2004. Superinfecting mycobacteria home to established tuberculous granulomas. *Nat. Immunol.* **5**:828–835.
- Cosma, C. L., K. Klein, R. Kim, D. Beery, and L. Ramakrishnan. 2006. *Mycobacterium marinum* Erp is a virulence determinant required for cell wall integrity and intracellular survival. *Infect. Immun.* **74**:3125–3133.
- Czuprynski, C. J., and A. K. Sample. 1990. Interactions of *Haemophilus-Actinobacillus-Pasteurella* bacteria with phagocytic cells. *Can. J. Vet. Res.* **54**(Suppl.):S36–S40.
- Dannenberg, A. M., Jr. 2006. Pathogenesis of human pulmonary tuberculosis. ASM Press, Washington, DC.
- Davis, J. M., H. Clay, J. L. Lewis, N. Ghori, P. Herbomel, and L. Ramakrishnan. 2002. Real-time visualization of *Mycobacterium*-macrophage interactions leading to initiation of granuloma formation in zebrafish embryos. *Immunity* **17**:693–702.
- DiRita, V. J., and J. J. Mekalanos. 1989. Genetic regulation of bacterial virulence. *Annu. Rev. Genet.* **23**:455–482.
- Dobos, K. M., F. D. Quinn, D. A. Ashford, C. R. Horsburgh, and C. H. King. 1999. Emergence of a unique group of necrotizing mycobacterial diseases. *Emerg. Infect. Dis.* **5**:367–378.
- Dulin, M. P. 1979. A review of tuberculosis (mycobacteriosis) in fish. *Vet. Med. Small Anim. Clin.* **74**:731–735.
- Eissenberg, L. G., S. Poirier, and W. E. Goldman. 1996. Phenotypic variation and persistence of *Histoplasma capsulatum* yeasts in host cells. *Infect. Immun.* **64**:5310–5314.
- El-Etr, S. H., S. Subbian, S. L. Cirillo, and J. D. Cirillo. 2004. Identification of two *Mycobacterium marinum* loci that affect interactions with macrophages. *Infect. Immun.* **72**:6902–6913.
- El-Etr, S. H., L. Yan, and J. D. Cirillo. 2001. Fish monocytes as a model for mycobacterial host-pathogen interactions. *Infect. Immun.* **69**:7310–7317.
- Frehel, C., A. Ryter, N. Rastogi, and H. David. 1986. The electron-transparent zone in phagocytized *Mycobacterium avium* and other mycobacteria: formation, persistence and role in bacterial survival. *Ann. Inst. Pasteur Microbiol.* **137B**:239–257.
- Gao, L. Y., R. Groger, J. S. Cox, S. M. Beverley, E. H. Lawson, and E. J. Brown. 2003. Transposon mutagenesis of *Mycobacterium marinum* identifies a locus linking pigmentation and intracellular survival. *Infect. Immun.* **71**:922–929.
- Gao, L. Y., S. Guo, B. McLaughlin, H. Morisaki, J. N. Engel, and E. J. Brown. 2004. A mycobacterial virulence gene cluster extending RD1 is required for cytolysis, bacterial spreading and ESAT-6 secretion. *Mol. Microbiol.* **53**:1677–1693.
- Gao, L. Y., F. Laval, E. H. Lawson, R. K. Groger, A. Woodruff, J. H. Morisaki, J. S. Cox, M. Daffe, and E. J. Brown. 2003. Requirement for *kasB* in *Mycobacterium mycolic acid biosynthesis, cell wall impermeability and intracellular survival: implications for therapy.* *Mol. Microbiol.* **49**:1547–1563.
- Gao, L. Y., M. Pak, R. Kish, K. Kajihara, and E. J. Brown. 2006. A mycobacterial operon essential for virulence in vivo and invasion and intracellular persistence in macrophages. *Infect. Immun.* **74**:1757–1767.
- Glomski, I. J., J. P. Corre, M. Mock, and P. L. Goossens. 2007. Cutting edge: IFN-gamma-producing CD4 T lymphocytes mediate spore-induced immunity to capsulated *Bacillus anthracis*. *J. Immunol.* **178**:2646–2650.
- Glover, N., A. Holtzman, T. Aronson, S. Froman, O. G. W. Berlin, P. Dominguez, K. A. Kunkel, G. Overturf, G. Stelma, Jr., C. Smith, and M. Yakus. 1994. The isolation and identification of *Mycobacterium avium* complex (MAC) recovered from Los Angeles potable water, a possible source of infection in AIDS patients. *Int. J. Environ. Health Res.* **4**:63–72.
- Gluckman, S. J. 1995. *Mycobacterium marinum*. *Clin. Dermatol.* **13**:273–276.
- Good, M. C., A. E. Greenstein, T. A. Young, H. L. Ng, and T. Alber. 2004. Sensor domain of the *Mycobacterium tuberculosis* receptor Ser/Thr protein kinase, PknD, forms a highly symmetric beta propeller. *J. Mol. Biol.* **339**: 459–469.

43. Grange, J. M. 1991. Environmental mycobacteria and human disease. *Lepr. Rev.* **62**:353–361.
44. Greenstein, A. E., J. A. MacGurn, C. E. Baer, A. M. Falick, J. S. Cox, and T. Alber. 2007. *Mycobacterium tuberculosis* Ser/Thr protein kinase D phosphorylates an anti-sigma factor homolog. *PLoS Pathog.* **3**:e49.
45. Groskop, J. A., and M. M. Brent. 1964. The effects of selected strains of pigmented microorganisms on small free-living amoebae. *Can. J. Microbiol.* **10**:579–584.
46. Hartman, J. L. T., B. Garvik, and L. Hartwell. 2001. Principles for the buffering of genetic variation. *Science* **291**:1001–1004.
47. Heifets, L. B., and R. C. Good. 1994. Current laboratory methods for the diagnosis of tuberculosis, p. 85–110. In B. R. Bloom (ed.), *Tuberculosis: pathogenesis, protection, and control*. ASM Press, Washington, DC.
48. Huang, X. Z., and L. E. Lindler. 2004. The pH6 antigen is an antiphagocytic factor produced by *Yersinia pestis* independent of *Yersinia* outer proteins and capsule antigen. *Infect. Immun.* **72**:7212–7219.
49. Huminer, D., S. D. Pitlik, C. Block, L. Kaufman, S. Amit, and J. B. Rosenfeld. 1986. Aquarium-borne *Mycobacterium marinum* skin infection: report of a case and review of the literature. *Arch. Dermatol.* **122**:698–703.
50. Irani, M., L. Orosz, S. Busby, T. Taniguchi, and S. Adhya. 1983. Cyclic AMP-dependent constitutive expression of gal operon: use of repressor titration to isolate operator mutations. *Proc. Natl. Acad. Sci. USA* **80**:4775–4779.
51. Jadin, J. B. 1975. Amibes limax vecteurs possible de Mycobacteries et de *M. leprae*. *Acta Leprol.* **59**:57–67.
52. Krishna-Prasad, B. N., and S. K. Gupta. 1978. Preliminary report on engulfment and retention of mycobacteria by trophozoites of axenically grown *Acanthamoeba castellanii* Douglas. *Curr. Sci.* **47**:245–247.
53. Laughon, A., and R. F. Gesteland. 1982. Isolation and preliminary characterization of the *GAL4* gene, a positive regulator of transcription in yeast. *Proc. Natl. Acad. Sci. USA* **79**:6827–6831.
54. Lee, C. A., B. D. Jones, and S. Falkow. 1992. Identification of a *Salmonella typhimurium* invasion locus by selection for hyperinvasive mutants. *Proc. Natl. Acad. Sci. USA* **89**:1847–1851.
55. Lemassu, A., A. Ortalo-Magne, F. Bardou, G. Silve, M. A. Laneelle, and M. Daffe. 1996. Extracellular and surface-exposed polysaccharides of non-tuberculous mycobacteria. *Microbiology* **142**(Pt. 6):1513–1520.
56. Lenaerts, A. J., D. Hoff, S. Aly, S. Ehlers, K. Andries, L. Cantarero, I. M. Ormae, and R. J. Basaraba. 2007. Location of persisting mycobacteria in a guinea pig model of tuberculosis revealed by R207910. *Antimicrob. Agents Chemother.* **51**:3338–3345.
57. Linell, E., and A. Norden. 1954. *Mycobacterium balnei*: new acid-fast bacillus occurring in swimming pools and capable of producing skin lesions in humans. *Acta Tuberc. Scand.* **33**:1–84.
58. Locke, J. B., K. M. Colvin, A. K. Datta, S. K. Patel, N. N. Naidu, M. N. Neely, V. Nizet, and J. T. Buchanan. 2007. *Streptococcus iniae* capsule impairs phagocytic clearance and contributes to virulence in fish. *J. Bacteriol.* **189**:1279–1287.
59. Long, E. R. 1958. The chemistry and chemotherapy of tuberculosis, 3rd ed. The Williams & Wilkins Co., Baltimore, MD.
60. Luong, T. T., and C. Y. Lee. 2002. Overproduction of type 8 capsular polysaccharide augments *Staphylococcus aureus* virulence. *Infect. Immun.* **70**:3389–3395.
61. Lurie, M. B. 1964. Resistance to tuberculosis: experimental studies in native and acquired defensive mechanisms. Harvard University Press, Cambridge, MA.
62. Lurie, M. B., P. Zappasodi, and C. Tickner. 1955. On the nature of genetic resistance to tuberculosis in the light of the host-parasite relationships in natively resistant and susceptible rabbits. *Am. Rev. Tuberc.* **72**:297–329.
63. Maniar, A. C., and L. R. Vanbuckethout. 1976. *Mycobacterium kansasii* from an environmental source. *Can. J. Public Health* **67**:59–60.
64. Marchler-Bauer, A., J. B. Anderson, C. DeWeese-Scott, N. D. Fedorova, L. Y. Geer, S. He, D. I. Hurwitz, J. D. Jackson, A. R. Jacobs, C. J. Lanczycki, C. A. Liebert, C. Liu, T. Madej, G. H. Marchler, R. Mazumder, A. N. Nikolskaya, A. R. Panchenko, B. S. Rao, B. A. Shoemaker, V. Simonyan, J. S. Song, P. A. Thiessen, S. Vasudevan, Y. Wang, R. A. Yamashita, J. J. Yin, and S. H. Bryant. 2003. CDD: a curated Entrez database of conserved domain alignments. *Nucleic Acids Res.* **31**:383–387.
65. McDonough, K. A., M. A. Florczyk, and Y. Kress. 2000. Intracellular passage within macrophages affects the trafficking of virulent tubercle bacilli upon reinfection of other macrophages in a serum-dependent manner. *Tuberc. Lung Dis.* **80**:259–271.
66. Mehta, P. K., A. K. Pandey, S. Subbian, S. H. El-Etr, S. L. Cirillo, M. M. Samrakandi, and J. D. Cirillo. 2006. Identification of *Mycobacterium marinum* macrophage infection mutants. *Microb. Pathog.* **40**:139–151.
67. Mekalanos, J. J. 1992. Environmental signals controlling expression of virulence determinants in bacteria. *J. Bacteriol.* **174**:1–7.
68. Miller, J. F., J. J. Mekalanos, and S. Falkow. 1989. Coordinate regulation and sensory transduction in the control of bacterial virulence. *Science* **243**:916–922.
69. Mor, N. 1985. Multiplication of *Mycobacterium marinum* within phagolysosomes of murine macrophages. *Infect. Immun.* **48**:850–852.
70. Moura, A. C., and M. Mariano. 1990. Dead *Mycobacterium leprae* inhibits phagocytosis by inflammatory macrophages in vivo: participation of the bacteria cell lipids in the phenomenon. *Mem. Inst. Oswaldo Cruz* **85**:381–382.
71. Moura, A. C., and M. Mariano. 1996. Lipids from *Mycobacterium leprae* cell wall are endowed with an anti-inflammatory property and inhibit macrophage function in vivo. *Immunology* **89**:613–618.
72. Moura, A. C., M. Modolell, and M. Mariano. 1997. Down-regulatory effect of *Mycobacterium leprae* cell wall lipids on phagocytosis, oxidative respiratory burst, and tumour cell killing by mouse bone marrow-derived macrophages. *Scand. J. Immunol.* **46**:500–505.
73. Nigrelli, R. F., and H. Vogel. 1963. Spontaneous tuberculosis in fishes and in other cold-blooded vertebrates with special reference to *Mycobacterium fortuitum* Cruz from fish and human lesions. *Zoologica* **48**:131–144.
74. Norden, A., and F. Linell. 1951. A new type of pathogenic *Mycobacterium*. *Nature* **168**:826.
75. Ortalo-Magne, A., M. A. Dupont, A. Lemassu, A. B. Andersen, P. Gounon, and M. Daffe. 1995. Molecular composition of the outermost capsular material of the tubercle bacillus. *Microbiology* **141**(Pt. 7):1609–1620.
76. Ortalo-Magne, A., A. Lemassu, M. A. Laneelle, F. Bardou, G. Silve, P. Gounon, G. Marchal, and M. Daffe. 1996. Identification of the surface-exposed lipids on the cell envelopes of *Mycobacterium tuberculosis* and other mycobacterial species. *J. Bacteriol.* **178**:456–461.
77. O'Sullivan, D. J., S. A. Walker, S. G. West, and T. R. Klaenhammer. 1996. Development of an expression strategy using a lytic phage to trigger explosive plasmid amplification and gene expression. *Bio/Technology* **14**:82–87.
78. Pagan-Ramos, E., S. S. Master, C. L. Pritchett, R. Reimschuessel, M. Trucksis, G. S. Timmins, and V. Deretic. 2006. Molecular and physiological effects of mycobacterial *oxyR* inactivation. *J. Bacteriol.* **188**:2674–2680.
79. Pagan-Ramos, E., J. Song, M. McFalone, M. H. Mudd, and V. Deretic. 1998. Oxidative stress response and characterization of the *oxyR-ahpC* and *furA-katG* loci in *Mycobacterium marinum*. *J. Bacteriol.* **180**:4856–4864.
80. Perez, J., R. Garcia, H. Bach, J. H. de Waard, W. R. Jacobs, Jr., Y. Av-Gay, J. Bubis, and H. E. Takiff. 2006. *Mycobacterium tuberculosis* transporter MmpL7 is a potential substrate for kinase PknD. *Biochem. Biophys. Res. Commun.* **348**:6–12.
81. Ramakrishnan, L., and S. Falkow. 1994. *Mycobacterium marinum* persists in cultured mammalian cells in a temperature-restricted fashion. *Infect. Immun.* **62**:3222–3229.
82. Ramakrishnan, L., N. A. Federspiel, and S. Falkow. 2000. Granuloma-specific expression of *Mycobacterium* virulence proteins from the glycine-rich PE-PGRS family. *Science* **288**:1436–1439.
83. Ramakrishnan, L., H. T. Tran, N. A. Federspiel, and S. Falkow. 1997. A *crbB* homolog essential for photochromogenicity in *Mycobacterium marinum*: isolation, characterization, and gene disruption via homologous recombination. *J. Bacteriol.* **179**:5862–5868.
84. Ramakrishnan, L., R. H. Valdivia, J. H. McKerrow, and S. Falkow. 1997. *Mycobacterium marinum* causes both long-term subclinical infection and acute disease in the leopard frog (*Rana pipiens*). *Infect. Immun.* **65**:767–773.
85. Ridenour, D. A., S. L. Cirillo, S. Feng, M. M. Samrakandi, and J. D. Cirillo. 2003. Identification of a gene that affects the efficiency of host cell infection by *Legionella pneumophila* in a temperature-dependent fashion. *Infect. Immun.* **71**:6256–6263.
86. Robinson, N., M. Wolke, K. Ernestus, and G. Plum. 2007. A mycobacterial gene involved in synthesis of an outer cell envelope lipid is a key factor in prevention of phagosome maturation. *Infect. Immun.* **75**:581–591.
87. Rousseau, C., O. Neyrolles, Y. Bordat, S. Giroux, T. D. Sirakova, M. C. Prevost, P. E. Kolattukudy, B. Gicquel, and M. Jackson. 2003. Deficiency in mycolipenate- and mycosanoate-derived acyltrehaloses enhances early interactions of *Mycobacterium tuberculosis* with host cells. *Cell Microbiol.* **5**:405–415.
88. Ruley, K. M., J. H. Ansed, C. L. Pritchett, A. M. Talaat, R. Reimschuessel, and M. Trucksis. 2004. Identification of *Mycobacterium marinum* virulence genes using signature-tagged mutagenesis and the goldfish model of mycobacterial pathogenesis. *FEMS Microbiol. Lett.* **232**:75–81.
89. Ruley, K. M., R. Reimschuessel, and M. Trucksis. 2002. Goldfish as an animal model system for mycobacterial infection. *Methods Enzymol.* **358**:29–39.
90. Scorpio, A., D. J. Chabot, W. A. Day, D. K. O'Brien, N. J. Vietri, Y. Itoh, M. Mohamadzadeh, and A. M. Friedlander. 2007. Poly- γ -glutamate capsule-degrading enzyme treatment enhances phagocytosis and killing of encapsulated *Bacillus anthracis*. *Antimicrob. Agents Chemother.* **51**:215–222.
91. Shimoji, Y., Y. Yokomizo, T. Sekizaki, Y. Mori, and M. Kubo. 1994. Presence of a capsule in *Erysipelothrix rhusiopathiae* and its relationship to virulence for mice. *Infect. Immun.* **62**:2806–2810.
92. Solomon, J. M., G. S. Leung, and R. R. Isberg. 2003. Intracellular replication of *Mycobacterium marinum* within *Dicyostelium discoideum*: efficient replication in the absence of host coronin. *Infect. Immun.* **71**:3578–3586.
93. Stokes, R. W., R. Norris-Jones, D. E. Brooks, T. J. Beveridge, D. Doxsee, and L. M. Thorson. 2004. The glycan-rich outer layer of the cell wall of *Mycobacterium tuberculosis* acts as an antiphagocytic capsule limiting the

- association of the bacterium with macrophages. *Infect. Immun.* **72**:5676–5686.
94. **Stolt, P., and N. G. Stoker.** 1996. Functional definition of regions necessary for replication and incompatibility in the *Mycobacterium fortuitum* plasmid pAL5000. *Microbiology* **142**:2795–2802.
 95. **Subbian, S., P. K. Mehta, S. L. Cirillo, L. E. Bermudez, and J. D. Cirillo.** 2007. A *Mycobacterium marinum mel2* mutant is defective for growth in macrophages that produce reactive oxygen and reactive nitrogen species. *Infect. Immun.* **75**:127–134.
 96. **Subbian, S., P. K. Mehta, S. L. Cirillo, and J. D. Cirillo.** 2007. The *Mycobacterium marinum mel2* locus displays similarity to bacterial bioluminescence systems and plays a role in defense against reactive oxygen and nitrogen species. *BMC Microbiol.* **7**:4.
 97. **Swaim, L. E., L. E. Connolly, H. E. Volkman, O. Humbert, D. E. Born, and L. Ramakrishnan.** 2006. *Mycobacterium marinum* infection of adult zebra fish causes caseating granulomatous tuberculosis and is moderated by adaptive immunity. *Infect. Immun.* **74**:6108–6117.
 98. **Tan, T., W. L. Lee, D. C. Alexander, S. Grinstein, and J. Liu.** 2006. The ESAT-6/CFP-10 secretion system of *Mycobacterium marinum* modulates phagosome maturation. *Cell Microbiol.* **8**:1417–1429.
 99. **Ulrichs, T., and S. H. Kaufmann.** 2006. New insights into the function of granulomas in human tuberculosis. *J. Pathol.* **208**:261–269.
 100. **Ulrichs, T., M. Lefmann, M. Reich, L. Morawietz, A. Roth, V. Brinkmann, G. A. Kosmiadi, P. Seiler, P. Aichele, H. Hahn, V. Krenn, U. B. Gobel, and S. H. Kaufmann.** 2005. Modified immunohistological staining allows detection of Ziehl-Neelsen-negative *Mycobacterium tuberculosis* organisms and their precise localization in human tissue. *J. Pathol.* **205**:633–640.
 101. **van Duijn, C.** 1981. Tuberculosis in fish. *J. Small Anim.* **22**:391–411.
 102. **von Reyn, C. F., J. N. Maslow, T. W. Barber, J. O. Falkinham, III, and R. D. Arbeit.** 1994. Persistent colonization of potable water as a source of *Mycobacterium avium* infection in AIDS. *Lancet* **343**:1137–1141.
 103. **von Reyn, C. F., R. D. Waddell, T. Eaton, R. D. Arbeit, J. N. Maslow, T. W. Barber, R. J. Brindle, C. F. Gilks, J. Lumio, J. Lähdevirta, A. Ranki, D. Dawson, and J. O. Falkinham, III.** 1993. Isolation of *Mycobacterium avium* complex from water in the United States, Finland, Zaire, and Kenya. *J. Clin. Microbiol.* **31**:3227–3230.
 104. **Wendt, S. L., K. L. George, B. C. Parker, H. Gruft, and J. O. Falkinham, III.** 1980. Epidemiology of infection by nontuberculous mycobacteria: isolation of potentially pathogenic mycobacteria from aerosols. *Am. Rev. Respir. Dis.* **122**:259–263.
 105. **Whitnack, E., A. L. Bisno, and E. H. Beachey.** 1981. Hyaluronate capsule prevents attachment of group A streptococci to mouse peritoneal macrophages. *Infect. Immun.* **31**:985–991.
 106. **Yip, M. J., J. L. Porter, J. A. Fyfe, C. J. Lavender, F. Portaels, M. Rhodes, H. Kator, A. Colorni, G. A. Jenkin, and T. Stinear.** 2007. Evolution of *Mycobacterium ulcerans* and other mycolactone-producing mycobacteria from a common *Mycobacterium marinum* progenitor. *J. Bacteriol.* **189**:2021–2029.

Editor: A. Camilli